| AD NUMBER |
| --- |
| **AD038783** |
| CLASSIFICATION CHANGES |
| TO: **unclassified** |
| FROM: **confidential** |
| LIMITATION CHANGES |
| TO:<br>**Approved for public release; distribution is unlimited.** |
| FROM:<br>**Distribution: Further dissemination only as directed by Office of Naval Research, code 466, Washington, DC, JUL 1954, or higher DoD authority.** |
| AUTHORITY |
| **31 jul 1966, DoDD 5200.10; ntis onr ltr, 26 oct 1977** |

| AD NUMBER |
| --- |
| **AD038783** |
| CLASSIFICATION CHANGES |
| TO:<br><br>**confidential** |
| FROM:<br><br>**secret** |
| AUTHORITY |
| **31 jul 1957, DoDD 5200.10** |

AD _____



# PROJECT MICHAEL

CONTRACT N6-ONR-27135

COLUMBIA UNIVERSITY

HUDSON LABORATORIES

DOBBS FERRY, N. Y.

RESEARCH SPONSORED BY

OFFICE OF NAVAL RESEARCH

CU-29-54-ONR-271-Phys

COLUMBIA UNIVERSITY

Hudson Laboratories

Dobbs Ferry, N. Y.

PROJECT MICHAEL

Contract N6-ONR-27135

Technical Report No. 22

# Shallow Water Studies Near St. Thomas, V.I.

by

Ivan Tolstoy, Roberto Frassetto and Leon P. Goldberg

W. A. Nierenberg
Director

Research Sponsored by
Office of Naval Research



Copy No. 055 SECRET

of 65 Copies July 20, 1954

This report consists of 66 pages

TABLE OF CONTENTS

LIST OF FIGURES

LIST OF FIGURES (Cont'd)

## SUMMARY

During the period from January 29 to February 17, 1954, a series of experiments were performed in water averaging 110 ft in depth in the vicinity of St. Thomas, V. I. These studies used an anchored buoy as a fixed reference point and consisted of a fathometer survey, two reversed refraction profiles and CW pressure field measurements canvassing the 10-35 cps band in 2 1/2 cps steps. The modified A Mark 6(b) acoustic minesweeping gear was used as a source. An AX-58 hydrophone, towed at speeds of 3 to 7 knots, was used for listening. In most cases, the noise level due to towing was sufficiently low to permit the recording of a usable signal out to ranges of 2000 to 4000 yds. A map of the pressure field was obtained at 20 cps exhibiting the influence of submarine topography. The salient result of these investigations was to substantiate the existence of peak pressure levels for a frequency of 25 cps, which is quite close to the Airy phase frequency as determined from shot data (20 1/2 cps). This verifies an earlier prediction made on the basis of normal mode theory.

# SHALLOW WATER STUDIES NEAR ST. THOMAS, V. I.

by

Ivan Tolstoy, Roberto Frassetto, Leon P. Goldberg

## I. GENERAL CONSIDERATIONS CONCERNING SHALLOW WATER CW MEASUREMENTS

Low frequency CW propagation in shallow water has received considerable attention in recent years because it is of practical importance for minesweeping and for passive and active submarine detection purposes.

In principle, one would like to know the characteristic properties of CW propagation in all shallow water areas of strategic interest, with particular reference to harbors, both domestic and foreign.

Comprehensive canvassing of all such areas by means of actual CW pressure field measurements appears to be an undertaking of impossible magnitude. Besides which, a great many locations are obviously inaccessible to us.

We shall therefore certainly have to rely upon a forecasting program that can be imagined to consist of the following steps:

a) Actual CW pressure field measurements in as many areas as possible.

b) The predicting of characteristics of CW propagation in areas of known bottom structure without the performance of time consuming CW experiments. This step presupposes a concurrent program for the purpose of determining bottom structure, (refraction shooting, dispersion studies and perhaps reflection work). The possibility of using narrow band filtering techniques with shot created transients for the direct determination of some of the properties of CW propagation should also be looked into.

c) Estimating the characteristics of CW propagation in areas of unknown bottom structure by means of educated guesses about that structure.

But before any predictions of the type b or c can be made, one must have a reliable method or theory by means of which to make such predictions from a knowledge of bottom structure. The standard theory of normal modes seems potentially capable of providing us with such a method. It has proved itself quite accurate and trustworthy in dealing with transient phenomena both in the field (shot work) and the laboratory (model work). A natural assumption to make is that it must work equally well under CW conditions. However, one must first establish beyond reasonable doubt that satisfactory correlation between theory and experiment is the rule, rather than the exception. But since the earth's geology is notoriously unpredictable in detail, and the idealized models that the physicist must use for computational purposes are rarely, if ever, encountered in practice, one must often be satisfied with agreement along general lines. The question that then arises is: for what type of phenomena is one justified in expecting good agreement between theory and experiment? In other words, given certain average bottom conditions, what will be the measurable fundamental properties of CW propagation least likely to disappear owing to details of local structure? Theory cannot resolve this question and an answer must be sought for in field experimentation. Such is the philosophy behind these shallow water CW experiments. They tell us how realistic an idealized model can be and what type of predictions may in general be based upon it.

## II. PURPOSE OF THE ST. THOMAS EXPERIMENT

The above discussion outlines the general purpose of the St. Thomas experiment. But, included under the general heading of comparison of theory and experiment, we set out to test one specific idea of considerable practical importance. In an earlier report[1] we had predicted the existence of resonant frequencies for CW work in layered media. Calculations showed that given a CW source whose frequency and amplitude could be varied so as to keep the power output constant, there existed frequencies for which the average pressure level at any range would be a maximum. In the two-layer case, these frequencies were found to be very close to the Airy frequency of each mode. We shall show how this phenomenon has been verified in the St. Thomas area.

Broadly speaking the St. Thomas experiments consisted of CW pressure field measurements and supporting investigations designed to give us the required bottom information. This supporting phase consisted of a fathometer survey and two reversed refraction profiles at right angles to each other.

The geographical center of all operations was a fixed buoy at $18^{\circ}$ 13 1/2' N, $65^{\circ}$ 02 1/2' W, approximately 6 1/2 miles southwest of Flamingo Point (Fig. 1).

## III. SUBMARINE TOPOGRAPHY OF SITE

The fathometer survey was carried out on January 29, 1954 by the USS ALLEGHENY (ATA179) with the use of a continuously recording EDO fathometer. The pattern of ships' courses is shown in Fig. 2. Radar ranges and bearings on the buoy were obtained every ten minutes. Figure 2 shows that the bottom slopes rather gently to the south until the 150 ft contour is reached about one mile south of the buoy, at which point it drops off very steeply to considerable depths south of the Virgin Islands platform.

A pronounced ridge (coral?) skirts the edge of this slope. These and other irregularities make it necessary to exercise caution in dealing with the interpretation of CW data. Thus it is hard to expect that runs taken to the SW of the buoy will be comparable to runs taken to the NE. The effect of this bottom topography on the CW pressure field will be described below.

## IV. SHOT WORK

Two reversed refraction lines at right angles to each other were shot on February 17 and 18, 1954. They came together at the buoy (Fig. 1). We thus obtained direct estimates of bottom velocity and layering by the usual travel time method. Information was also obtained from the study of water wave dispersion, Airy phase frequency and velocity, and frequencies of the ground waves.

All profiles were shot with the ALLEGHENY recording and anchored, and C.G. 506 as shooting ship. During each run the latter went out from the ALLEGHENY at 6-7 knots, shooting charges every two minutes. For recording, the output of a floated AX-58 hydrophone was led into an SIE camera and a Sanborn 4-channel recorder. The direct water wave and the radio time break were recorded on 500 cps high-pass rectified channels. The refracted waves were usually recorded best on a 2.5-25 cps band pass (Krohn-Hite filter) channel. Harmonics (higher modes) were found in the 40-100 cps and 60 cps low-pass channels.

Profile I was shot as follows: The Ia run was made with the ALLEGHENY anchored at the buoy, and C.G. 506 going off on a 336° true bearing. For Ib the ALLEGHENY anchored at a point 12,000 yards on a 336° true bearing from the buoy, the C.G. 506 going off on a 156° true bearing from the ALLEGHENY to the buoy. Thus Ia and Ib were reverses of each other.

Similarly IIa and IIb constituted reverses of each other for a line bearing 66° true from the buoy. In IIa the ALLEGHENY was recording at the buoy, and in IIb she was at a point 11,000 yds on a 67° true bearing from the buoy.

### 1. Travel Time Curves

The arrival times of the most prominent and consistent phases as functions of the direct water wave travel times (D) for lines Ia and b, IIa and b are shown respectively in Figs. 3, 4, 5, and 6. All lines shown are best fits in the least squares sense. The uncertainties refer to the 80% confidence limits as given by Student's t. The speed of sound in water was taken to be 5040 ft per sec consistently with a probable salinity of the order of 34 and a BT measurement showing a constant temperature of 80°.

Profile I

Ia shows a very bad scatter of points, (much greater than on any of the other lines). There are only two clearly identifiable series of arrivals giving the following velocities and intercepts:

$V_1 = 6630 \pm 350$ ft per sec $\qquad I_1 = .050 \pm .11$

$V_2 = 17200 \pm 2900$ ft per sec $\qquad I_2 = .48 \pm .14$

A few arrivals were seen that could, perhaps, represent a 5400-5600 layer ($V_m$) overlying the $V_1$ formation, but in insufficient number to give us a line.

Note that the scatter of points is such as to make the intercept of the $V_1$ arrival have no real significance.

Ib shows only doubtful $V_m$ and $V_1$ arrivals. For $V_2$ it gives:

$V_2 = 14160 \pm 330$ ft per sec $\qquad I_2 = .0025 \pm .04$

This intercept is such as to suggest that the $V_2$ layer here forms the sea floor.

Combining Ia and Ib we get:

Slope of $V_2$ layer towards buoy:

$$\theta_{V_2} = 1.7^\circ \pm 1.7$$

$$V_2 = 15500 \pm 1500 \text{ ft per sec.}$$

The only good evidence for $V_1$:

$$V_1 = 6630 \pm 350 \text{ ft per sec.}$$

Thickness of $V_1$ beneath the buoy:

$$h_1 = 1700 \pm 700 \text{ ft.}$$

A schematic cross section is shown in Fig. 7.

Profile II

IIa gives no conclusive evidence for $V_M$. The $V_1$ line presents an obvious break at a point corresponding to D≈2.2 sec. This suggests a discontinuity in bottom properties at a point two miles or so on a 66° true bearing from the buoy.

In close (D< 2.2 sec.):

$V_1 = 7630 \pm 300$ ft per sec $\qquad I_1 = .055 \pm .047$

Northeast of the dincontinuity (D> 2.2 sec.):

$V_1 = 6340 \pm 210$ ft per sec $\qquad I_1 = -0.11 \pm 0.11$

The intercept of the 7630 ft per sec $V_1$ layer near the buoy appears to be significantly different from zero (in the least squares 50% confidence limits the uncertainty would be roughly half, i.e. $I_1 = 0.055 \pm .024$). A thin intervening $V_M$ layer is therefore conceivable.

The underlying high velocity medium is:

$V_2 = 17300 \pm 600$ ft per sec $\qquad I_2 = .500 \pm .04.$

IIb furnishes conclusive evidence for the existence of a $V_M$ layer, probably directly beneath the water layer:

$V_M = 5460 \pm 160$ ft per sec $\qquad I_M = .08 \pm .14.$

The intercept does not differ significantly from zero. As in Ib, there is only poor evidence for $V_1$, but $V_2$ is well defined:

$V_2 = 14950 \pm 400$ ft per sec $\qquad I_2 = 0.10 \pm .04$

This intercept indicates that if $V_1$ is present at all at this end of Profile II, it is quite thin.

The interpretation of the above data gives:

Slope of $V_2$ layer (towards buoy):

$\theta = 1.37° \pm 0.($

$V_2 = 16020 \pm 530$ ft per sec.

Near the buoy:

$$V_1 = 7630 \pm 300 \text{ ft per sec.}$$

This layer has a thickness of

$$h_1 = 2090 \pm 250 \text{ ft.}$$

At the far end, about five miles from the buoy there is in addition an unconsolidated layer overlying $V_1$:

$$V_M = 5460 \pm 160 \text{ ft per sec}$$

about 300 ft thick.

If this layer is present near the buoy, its thickness is appreciably less than 300 ft. It could conceivably even be absent. A schematic cross section is shown in Fig. 7.

## 2. Dispersion Data

In a medium of variable acoustical parameters the propagation of sound is dispersive, i.e. the energies associated with different frequencies travel with different velocities (group velocity). The dispersion of transients (such as those created by explosives) in such media can yield considerable information concerning the acoustical structure of these media. Indeed, an ideal dispersion experiment should in principle completely and accurately describe the properties of the medium. Thus if we wanted to investigate the structure of a layered liquid or solid we could explode one charge and obtain an experimental dispersion curve (group velocity vs frequency). If we then had at our disposal a comprehensive collection of calculated dispersion curves designed to cover all possible field cases we could determine the local structure by finding the best fit to the experimental curve. This technique has obvious advantages. In the case of horizontal or nearly horizontal bottom stratification, it yields in one stroke all of the velocity and thickness data given by the standard travel time technique. It commands greater precision in dealing with thin near-surface layers. It gives us information that the travel time technique is intrinsically incapable of providing: thus it is potentially capable of giving the densities of the various layers, and it eliminates the large errors in the velocity determination of a given layer when this layer is thin compared to the wave lengths involved.

At the present time, there are obstacles to the wholesale use of this method, the most important of which is the absence of adequate dispersion tables. A complete discussion of the difficulties involved would be out of place in this report. It suffices to say that none of them appear to be insurmountable.

Insofar as the St. Thomas experiment is concerned, we have used the dispersion data to complement and fill out the travel time information.

Group Velocity of the Water Wave

In the Pekeris nomenclature, the whole dispersive wave train immediately following the direct water wave arrival is called the water wave. Figure 8 shows this wave train as recorded on Shot #8, line IIb. To obtain from it group velocity, U, as a function of frequency, f, we used the technique described by Pekeris,(2) which consists of taking one half the time interval between every other wave trough(or crest) as representing the period of the intervening trough (or crest). The ratio of arrival time of the direct water wave (of velocity $\alpha_1$), to that of this trough represents the ratio $U/\alpha_1$ for this period.

This analysis was performed for 10 shots, chosen for record clarity. The resulting plot of $U/\alpha_1$ vs f in cps is shown in Fig. 9. Because of bubble pulse interference, the useful frequency range is limited here to the 40-300 cps band.

The Airy Phase

An Airy phase may be defined as an arrival corresponding to a group velocity minimum. As such, it may be shown to correspond to relatively higher excitation amplitudes. Given a white source of waves in a layered medium, the effect of dispersion on a record may be compared to that of a broad band filter with a characteristic curve peaking in the vicinity of the Airy phase frequencies. A given mode of propagation in a liquid medium may be characterized by as many group velocity minima as there are layers of finite thickness (and possibly by twice as many in a layered solid).

The corresponding values of the frequencies and group velocities give us points on the dispersion curve. The position of these points is quite sensitive to all acoustical parameters involved, and may be diagnostic even in the absence of other dispersion data.

In the St. Thomas area, the Airy phase showed up quite clearly on a number of shots. An example is reproduced in Fig. 10.

A list of frequencies and group velocities for the Airy phase is shown in Table I.

TABLE I

| Shot Line | Shot No. | D* | Airy Phase Frequency | $U/\alpha_1$ |
|---|---|---|---|---|
| IIa | 6 | 2.36 sec | 18.5 cps | 0.86 |
| IIb | 3 | 1.43 | 20 | 0.88 |
| | 4 | 1.83 | 20 | 0.87 |
| | 5 | 2.15 | 21 | 0.89 |
| Ia | 2 | 0.764 | 23 | 0.81 |
| Ib | 3 | 1.702 | 20 | 0.82 |
| | 4 | 2.124 | 20 | 0.84 |
| Avg. | | | 20.4 | 0.85 |

We will utilize this average value to give us an additional point on our dispersion curve (Fig. 9).

## Ground Wave Frequencies

One or more points on the dispersion curve may always be secured by noting the frequencies of the "refracted waves" utilized in the travel time study. Thus, in the case of a low velocity layer over a semi-infinite liquid bottom (water over sediment), the possible frequencies of the bottom refracted wave are equal to the normal mode cutoff frequencies. In the case of three or more layers overlying a high velocity half-space, the frequencies of the refracted wave corresponding to this half-space are still the normal mode cutoff frequencies. But the "refracted arrivals" corresponding to intermediate layers are actually maxima of the group velocity curve. When such an intermediate layer is very thin, this maximum group velocity may not show up at all on the dispersion curves of the lower modes.

* Direct water wave travel time in seconds.

One has to go to the higher modes before this maximum becomes identifiable. This means that, in practice, unless one goes to relatively high frequencies, a thin intermediate layer may remain unidentified. If on the contrary such an intermediate layer is very thick, then one may, for all practical purposes, consider two distinct two-layer problems, and the refracted wave corresponding to the intermediate layer will not differ appreciably in frequency or velocity from the cutoff frequency obtained by considering this layer as being semi-infinite.

Table II shows a list of frequencies corresponding to the $V_1$ arrival.

TABLE II

| Shot Line | Shot No. | D | $V_1$ |
|---|---|---|---|
| IIa | 2 | 0.970 sec | 11.8 cps |
| | 3 | 1.299 | 11.0 |
| | 5 | 1.949 | 11.0 |
| | 7 | 2.610 | 12.5 |
| | 8 | 2.950 | 12.5 |
| Ia | 3 | 1.320 | 11.0 |
| | 5 | 1.683 | 12.5 |
| | 6 | 1.712 | 13.3 |
| | 7 | 2.350 | 13.3 |
| | 8 | 2.707 | 12.5 |

Note that the more distant shots tend to correspond to higher frequencies. This could correspond to the discontinuity in bottom velocity noted on the travel time curves.

We will look for a model giving a $V_1$ frequency between 11.0 and 13.0 cps to represent bottom conditions in the vicinity of the buoy.

## Fitting the Dispersion Data

After several tries at fitting these points to computed curves by means of the standard period equations,[2] we found two types of plane parallel layer models showing fair agreement.

1) The simplest was a two-layer model ignoring the possible presence of an unconsolidated mud layer (Fig. 11):

A layer of sea water of depth $h_1 = 122$ ft, sound velocity $d_1 = 5040$ ft per sec, density $\rho_1 = 1$, overlying a semi-infinite medium of sound velocity $\alpha_2 = V_1 = 7800$ ft per sec and density $\rho_2 = 1.5$.

Under these conditions the low frequency cutoff for the n'th mode is:

$$f_c = \frac{(2n-1)\alpha_1 \alpha_2}{4h_1\sqrt{\alpha_2^2 - \alpha_1^2}}$$

For $n = 1$ we have the frequency of the fundamental for the refracted arrival $V_1 = \alpha_2$:

$$f_{V_1} = 13.5 \text{ cps.}$$

The cutoff frequency for the second mode is then

$$f_c \ (n = 2) = 40.5 \text{ cps.}$$

For this model the fundamental Airy phase frequency and group velocity are:

$$f_A = 21.2 \text{ cps}$$

$$U = 0.91\alpha_1$$

This model has several defects, as may be seen from a comparison with the data of Tables I and II:

a) The predicted Airy phase group velocity and frequency are somewhat high.

b) The same holds true for the ground wave frequency. The computed group velocity curve is shown in Fig. 9 where it is labeled (1).

2) For the second model, three layers were postulated (Fig. 12), of sound velocities $\alpha_1 = 5040$ ft per sec, $\alpha_2 = 5544$ ft per sec, $\alpha_3 = 7600$ ft per sec; densities $\rho_1 = 1$, $\rho_2 = 2\rho_1$, $\rho_3 = 2.2\rho_1$; and thicknesses $h_1 = 100$ ft, $h_2 = 40$ ft. Insofar as the dispersion goes, the model should be numerically almost equivalent to taking a slightly thicker layer of water ($h_1 = 110$ ft) and thinner mud layer ($h_2 = 30$ ft) for example.

Solution of the period equation gives us:

Fundamental ground wave frequency:

$$f_{V_1} = 14.6 \text{ cps}$$

Second mode cutoff frequency:

$$f_c \ (n = 2) = 40.6 \text{ cps}$$

Airy phase frequency and group velocity:

$$f_A = 18.7 \text{ cps}$$

$$U = 0.871\alpha_1$$

For a water thickness of 125 ft and mud thickness of 50 ft the corresponding frequencies would be:

$$f_{V_1} = 11.7 \text{ cps}$$

$$f_c \ (n = 2) = 32.5 \text{ cps}$$

$$f_A = 15 \text{ cps}$$

Despite the better correspondence for the $V_1$ frequency of the latter case, the group velocity curve (curve (2), Fig. 9) indicates that a 100 ft layer of water overlying 40 ft of mud would more nearly approximate the average conditions, out to three or four miles from the buoy.

Despite the potentially greater promise of the three layer model no other hypotheses for the layering were investigated, in view of the length of the computations involved.

The efforts made in fitting the dispersion data to a reasonable theoretical model have borne forcefully to our attention the necessity for making large scale computations by machine methods. A fairly complete set of tables for two, three, four and five layer models would save enormous quantities of time in connection with any future work of this type.

## V. THE CW PRESSURE FIELD MEASUREMENTS

### 1. Instrumentation

#### The Source

The source used was the Navy A Mark 6(b) acoustic minesweeping gear, an electrically driven mechanical oscillator modified as described in an earlier report from this laboratory.[3] This unit consists of two opposed pistons each 27 in. in diameter which vibrate with an amplitude of either 1/8 in. or 1/2 in., depending on the crankshaft unit used in it. In lieu of interchanging crankshaft units, two A Mark 6(b) units were used, one with 1/8 in. piston displacement amplitude, the other with 1/2 in. amplitude. At large distances from the source, this unit acts effectively as a point source, the power output of which is proportional to $A^2f^4$; A being the amplitude and f the frequency. Thus the 1/2 in. amplitude unit will be used at the lower frequencies.

In an earlier field determination of the power output[4] it was estimated that with $A = 1/8$ in., $f = 30$ cps, the power output is of the order of 250 watts.

In the present experiment, modification of the control apparatus made it possible to vary the frequency of operation from 5 to 35 cps. This was accomplished by applying to the armature of the dc motor a rectified ac voltage which could be controlled by a 40 ampere variac. The frequency of the motor was monitored by applying a tachometer output signal to one set of plates of an oscilloscope and the output of a calibrated oscillator to the other set of plates. The resulting Lissajous pattern was manually maintained as steady as possible by adjusting the dc motor control. By this means the indicated off-frequency operation of the motor rarely exceeded 1/2 cycle per second and was no more than 1/5 of a cycle during most of the time. This could be determined by observing the changing pattern on the oscilloscope screen and measuring the time taken for the pattern to repeat itself. The reciprocal of this time interval is the frequency difference between the two signals being compared.

#### The Recording Gear

The pressure field was measured by a towed AX-58 Brush hydrophone, the output of which was fed through a tuned filter

amplifier with Q's of the order of 10 to 15, followed by a rectifier stage to an Esterline-Angus pen recorder. A block diagram is shown in Fig. 13.

In the absence of noise, the quantity recorded on the Esterline-Angus chart paper was thus the rms space envelope of the oscillating pressure field. Obviously, we wish to convert this trace into pressure units. To do this three types of calibration had to be made:

a) Calibration of the Recorder and Rectifier Unit. With two exceptions, the Esterline-Angus pen deflection was calibrated every day for a series of voltage inputs to the rectifier obtained with a microvolter and checked by a voltmeter. This procedure was necessary because the voltage corresponding to a given pen deflection was found to change somewhat from day to day.

b) Calibrations of Amplifiers were performed several times during the operation. The gain as a function of frequency for one amplifier is shown in Fig. 14. These results are probably reliable to $\pm$ 5%.

c) Calibration of the AX-58 Hydrophones. Three hydrophone calibrations were performed during the entire operation. One of these was a partial repeat, showing such absolute calibrations to be probably good to $\pm$ 10%. The procedure was to lower a calibrated Massa hydrophone taped to the AX-58 while the A Mark 6(b) was radiating. The outputs of the two were then recorded for from two to five minutes on the Esterline-Angus and compared for a series of frequencies. The resulting calibration in units of microvolts per dyne per $cm^2$ of one of the AX-58's used is shown in Fig. 15.

## The Towing Gear

A complete description of the hydrophone towing gear designed by R. Frassetto will be given upon completion of a series of tests now in progress.

It will suffice to note here that the towing system consisted of a towed float attached to the ship by rope and shock-cords, which dragged a heavy streamlined depressor pulling the hydrophone. The latter was enclosed in a streamlined casing which left the pressure sensitive nose free. The hydrophone cable was slack from depressor to float and from float to ship (Fig. 16). The hydrophone depth was estimated to be about 70 ft.

Numerous noise level determinations had to be made throughout the duration of the experiments. For this purpose during a given run (at some fixed frequency) the A Mark 6(b) would either be shut off or turned off frequency (by about 10 cps) for a two minute period. The resultant recording gave the noise level in equivalents of dynes per $cm^2$ for that particular course and time. In other cases, we have considered the noise level as being given by the average recorded level outside of the maximum range at which the signal could be heard at the end and/or beginning of a run. It is estimated that the noise level remained constant to within ± 10% of its average on a given run at constant speed, and was therefore treated as a constant for each run. To obtain the value of the CW pressure field this constant was subtracted from the level recorded by the Esterline-Angus. The noise level was of course a function of speed, frequency, ship's course and sea state. Rough curves for the average noise level as a function of speed at 15 and 20 cps are shown in Fig. 17. Observations at higher frequencies show a peak at 60 cps indicating electrical pickup. This cannot have contributed much to the background noise in this experiment since the frequencies investigated did not exceed 35 cps. The lowest noise in the 5-35 cps band seemed to occur at speeds of 5-7 knots, which were the highest available to us.

## 2. Procedure

The U.S.S. ALLEGHENY anchored each morning next to the fixed buoy and operated the A Mark 6(b) source. The latter's depth was kept constant at about 70 ft.

Two recording ships were used:

The RUBICON was a 70 ft ketch with diesel auxiliaries capable of doing speeds of 5-7 knots under power, and was used for towing the hydrophone. The C.G. 506 was inoperative most of the time. Towards the end of the program we obtained some rather scattered 20 and 15 cps long-range data while drifting.

The RUBICON followed straight line courses at constant speed towards and away from the ALLEGHENY, the A Mark 6(b) frequency being kept constant during each run. Navigational control was given by the ALLEGHENY'S radar by means of which fixes were obtained every ten minutes. The average relative accuracy of all runs is estimated to be ± 100 yds. Absolute errors with respect to the buoy are believed not to have exceeded 200 yds.

A total of 62 successful runs were made by the RUBICON at frequencies of 12.5 to 35 cps in the following proportions:

| Frequency (cps) | No. of Runs |
|---|---|
| 12.5 | 4 |
| 15 | 17 |
| 17.5 | 6 |
| 20 | 17 |
| 22.5 | 2 |
| 25 | 3 |
| 27.5 | 2 |
| 30 | 4 |
| 32.5 | 4 |
| 35 | 3 |

An Esterline-Angus tape for a typical 15 cps run is shown in Fig. 18.

## 3. Results

It is obvious that the amount of information was considerable. We had to limit ourselves to examining the following questions:

1. The influence of topography on the pressure field.
2. The Airy phase resonance effect.
3. The behaviour of the pressure field with range.

### Influence of Topography on the Pressure Field

At 20 cps a sufficient quantity of data was available to permit the drawing of CW level contours. Figure 19 shows the survey runs and Fig. 20 the resulting contour map of the pressure field. The influence of bottom topography is quite striking:

a) Broadly speaking there is an east-west stretching of the pressure contours following the regional east-west trend of the topographic contours. This suggests that in a plane sloping bottom the direction of optimum propagation would be parallel to the contours. Also, the pressure levels down-slope appear to be slightly higher than those up-slope.

b) There is a pressure ridge associated with the edge of the steep slope beginning 2000 or so yards south of the buoy. It could be due to either the presence of the (probably coral) ridge marking the lip of the slope, or to the presence of the slope itself, or to both. In principle, both of these features are capable of producing back-scattering of sound--just as in a wave guide changes in radiative impedance will result in partial reflection phenomena.

c) In general, one notes a tendency for pressure highs to be associated with topographic prominences. Thus, the sharpening and relative stretching of the western lobe of the pressure field is quite obviously associated with the topographic ridge coming in from the NW.

These results shed some light on the appropriate manner for handling the data. Thus to reduce the scatter of data due to topographic effects, one should preferably work in the first (NE) quadrant since the pressure field in it is relatively less disturbed by topographic effects.

## The Resonant Frequency

The majority of our runs were made in the NE and SW quadrants. These two quadrants are quite different from the standpoint of bottom topography, and we have seen that this has a marked influence upon the pressure field. For this reason, we have made comparisons between the runs for each quadrant separately.

Since the NE quadrant appears to have a smoother and more nearly horizontal bottom, we would expect the corresponding data to be perhaps more reliable.

The following comparisons of pressure levels have been made:

a) In Fig. 21, we show the smoothed out pressure level vs range curves on a log-log scale for 20, 22.5, 25, 30, 35 cps for neighboring runs in the NE quadrant. The corresponding ship's tracks are shown in solid lines in Fig. 22.

Figure 21 shows that the <u>average</u> pressure level from a few hundred yds on out is highest for frequencies of the order of 25 cps. For ranges exceeding 750 yds, the pressure level at any given range is consistently highest at 25 cps.

b) Figure 23 shows the pressure level at 1000 yds as a function of frequency for neighboring tracks in the NE quadrant (Fig. 22).

c) Figure 24 shows the average of the pressure levels at 750, 1000, 1250 yds for the same runs

d) Figure 25 shows the average of the pressure levels at 750, 1000, 1250 yds for neighboring runs in the SW quadrant as compared to those in the NE quadrant. The corresponding ship's tracks are also shown in Fig. 22.

All these curves show a pronounced peak at about 25 cps, which is effectively very close to the Airy phase frequency as determined from shot data. This is the predicted resonance effect. The observed phenomenon is considerably sharper than that predicted on the basis of any reasonable model. The reason for this sharpening is not understood at present. We believe it may be due to a combination of topographic and structural effects. The bottom structure in this area is not simple and the refraction data only give us a crude average picture of it. Marked local departures from any predictions based upon such a picture are therefore to be expected. Thus the introduction of an ad hoc high velocity layer such as a lava flow in the vicinity of the buoy could produce a very sharp peaking of the response curves.

The second peak occurring near 32.5 cps would be due to the appearance of the second mode.

Pressure-Range Curves

Figures 26, 27, 28, 29, 30, 31, 32, 33 show a series of pressure level vs range curves corresponding to the courses shown in Fig. 34. Figure 35 shows some of the runs corresponding to Fig. 21 on a semi-log scale. These are the curves shown also in Fig. 21, but they have not been smoothed out.

In general, the irregularities of these curves are not easy to explain. Comparison of courses very close together, such as Runs (1) and (2) for 20 cycles (Figs. 28, 29 and 35) shows that the major bumps and troughs are real features.

All log-log plots shown suggest an $R^{-1}$ to $R^{-3/2}$ pressure amplitude fall-off for moderate ranges. We suspect that the very rapid apparent fall-offs at ranges of more than

2500-3000 yds are due to noise effects (Fig. 36). When the noise and signal become comparable our method of subtracting a rectified noise-level from a rectified signal plus noise level becomes incorrect and will yield too low a figure for the signal level. This is illustrated by Fig. 36 in which we have plotted signal levels as determined by the C.G. 506 at large ranges, in approximately the same azimuth as the RUBICON Runs (1) and (2).

The semi-log plot of Fig. 35 shows that a good fit to the observed fall-off is obtained by an $e^{-R}$ law. This could be due to the relatively high velocity $V_2$ layer having a rigidity different from zero. Since the velocity of compressional waves is of the order of 7600 ft per sec, the velocity of shear waves would probably be less than the speed of sound in the liquid. There would then not be any truly unattenuated modes and all frequencies would suffer exponential attenuation. It is unfortunately impossible to test this idea quantitatively without a knowledge of Poisson's ratio for the $V_2$ layer.

Finally, we note that the 35 cps run (Fig. 33) shows considerable structure. This is due to the appearance at frequencies above 30 cps or so of the second undamped mode of the Pekeris theory, which would also be responsible for the second peak in the pressure level vs frequency curves. In an earlier report from this laboratory[4] describing some CW shallow water experiments in Long Island Sound, it was shown how structure of this kind could be explained by the superposition of two or more modes. In that report, it was also shown that the detail of these pressure-range curves is very sensitive to small changes of thickness of the mud layer. In view of this we have not attempted to fit the St. Thomas results to calculated pressure-range curves.

## Accuracy of Results

The main limiting factor on the accuracy of our pressure measurements was the noise generated by the towing of the hydrophone. Repeat runs such as those shown for 20 cps in Fig. 36 indicate that the measurements are reproducible on the average to within ± 20% at ranges less than 2000 yds. At larger ranges we have already noted a sudden decrease in signal level from Fig. 35. It is seen that simultaneously the reproducibility of the data decreases. This would be due to random phase relationships between noise and signal which cannot be easily taken into account following filtering and rectification.

The data gathered in St. Thomas can thus be considered as good to 20% for ranges not exceeding 2000-3000 yds, depending upon the frequency and noise level, since the calibration of all recording equipment was certainly not affected by errors of this magnitude.

## CONCLUSIONS

The St. Thomas experiment may be said to have achieved the following results:

1. The predicted "resonant" property of the Airy phase frequency has been verified experimentally.

2. The importance of variations in water depth of the order of 10-20% of the total depth has been shown.

3. A mew method of doing CW surveys while underway has proved feasible, thanks to a hydrophone towing system designed by R. Frassetto which allows speeds in excess of 5 knots.

4. As observed in a number of prior experiments [4,5] the pressure amplitude decreases with range considerably faster than predicted by theory. The decay law seems to be of the order of $R^{-1}$ to $R^{-3/2}$.

The first result is of obvious practical importance, in that it tells us something about the optimum frequency range to be used both in acoustic minesweeping in shallow waters and in narrow band listening devices. The fact that this frequency can be determined by the recording of a single explosive shot on location is worthwhile noting, since this means that elaborate CW surveys are not necessary for determining it.

The second result illustrates the desirability of further surveys of the type of our 20 cps survey. The chances are that our knowledge of the influence of bottom irregularities on the pressure field will have to depend upon such surveys, since a satisfactory theoretical treatment of the problem is not available. It also shows the necessity for conducting several more CW experiments in locations of flat bottom topography and simple structure.

The third result is most encouraging for the future execution of CW experiments, since it more or less guarantees

that we will be able to obtain satisfactory data in sufficient quantity for any chosen location. The towing system is now being perfected in order to increase our effective listening range.

As for the fourth result, we have pointed out that an exponential decay with range might perhaps give a better empirical fit to the smoothed pressure-range curves. The results of the U. S. Navy Mine Countermeasures Station group in Panama City[6] giving an $R^{-1/2}$ decay for ranges of 100 to 500 yds are not necessarily in contradiction with ours. For such small ranges an inspection of Figs. 21 and 36 will show that for many runs this approximation would be acceptable.

Excepting this last and by no means unusual[4,5] result, we can say that there is good qualitative agreement between theory and experiment. Quantitative agreement was hampered by topographic and lithological irregularities in the bottom, and the ensuing lack of precise information concerning bottom structure in the immediate vicinity of the buoy.

## REFERENCES

1. Tolstoy, I., Levin, F. K., and Frosch, R. A. Approaches to studies of shallow water sound propagation. Columbia University, Hudson Laboratories. December 10, 1953. Also appears as Appendix to Columbia University, Hudson Laboratories, Technical Report No. 21, A progress report in shallow water research. June 30, 1954.

2. Pekeris, C. L. Theory of propagation of explosive sound in shallow water, In The Geological Society of America, Memoir 27. New York, October 15, 1948.

3. Beck, H. C. and Sonnemann, H. Conversion of the A Mark 6(b) minesweeping gear to a 30 cycle sound source. Columbia University, Hudson Laboratories, Technical Report No. 8. February 10, 1953.

4. Becker, G. E., Carlson, R. O., Frosch, R. A., and Poss, H. L. 30 cps sound propagation in shallow water. Columbia University, Hudson Laboratories, Technical Report No. 9. April 15, 1953.

5. Becker, G. E., and Carlson, R. O. 15 & 30 cps sound propagation at a location near the entrance to New York harbor. Columbia University, Hudson Laboratories, Technical Report No. 13. October 15, 1953.

6. Elliott, M. E., Melchor, J. L., Young, J. M. Underwater sound transmission at low frequencies in St. Andrew Bay. U. S. Navy Mine Countermeasures Station, Report No. 26. April, 1950.

ACKNOWLEDGEMENTS

The field party conducting these studies, in addition to the authors, also included Drs. N. S. Shiren, M. V. Brown, L. Grabner (scientists) and M. Lomask, F. Macey, and A. Rose (technicians). The cooperation of these individuals was invaluable, as was the help of the officers and men of the USS ALLEGHENY and the St. Thomas Coast Guard Station. The cooperation of Mr. John Northrop in preparing the submarine topography map shown in Fig. 2 was greatly appreciated.

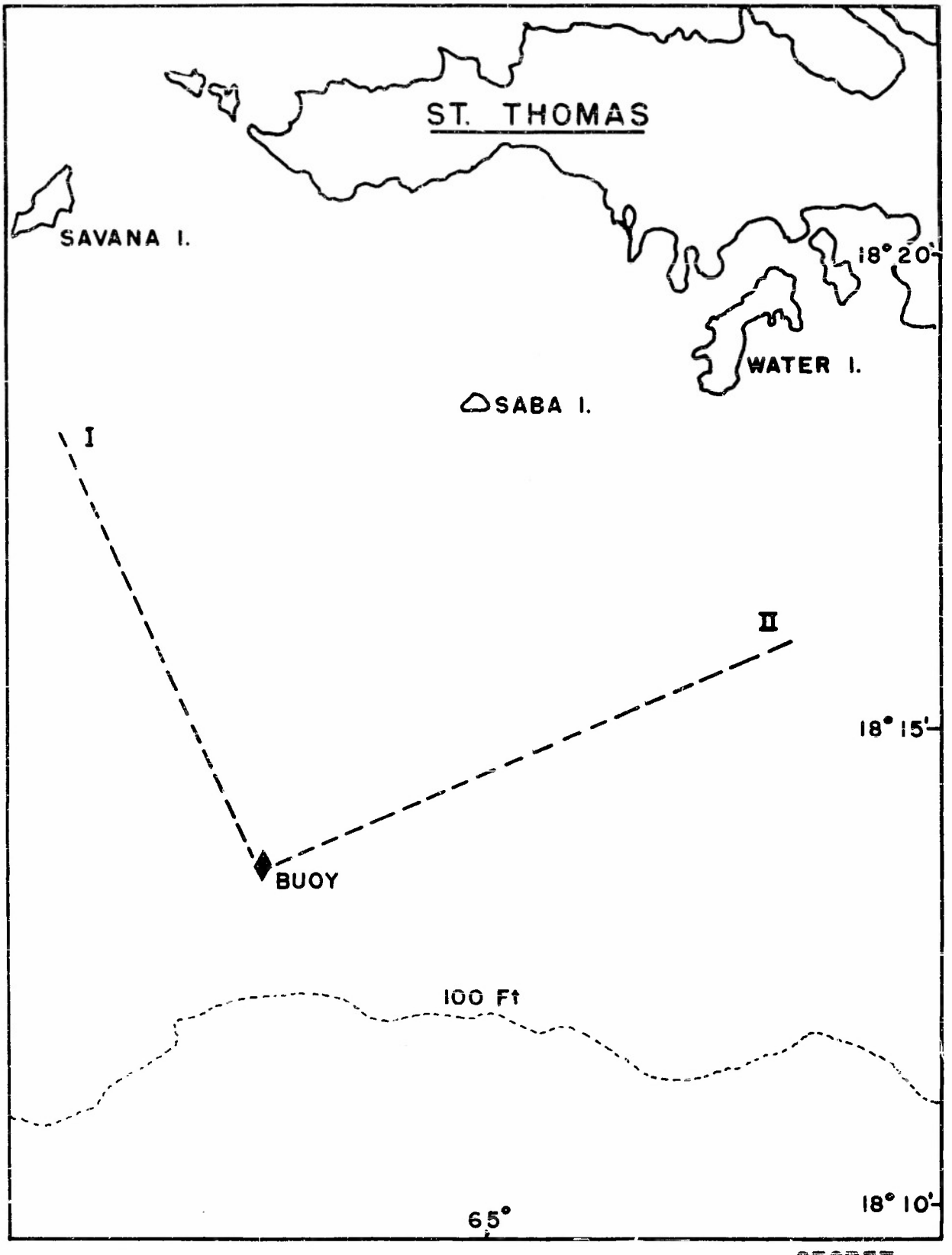
ST. THOMAS
SAVANA I.
18° 20'
WATER I.
SABA I.
I
II
18° 15'
BUOY
100 Ft
18° 10'
65°
SECRET

FIG. 1

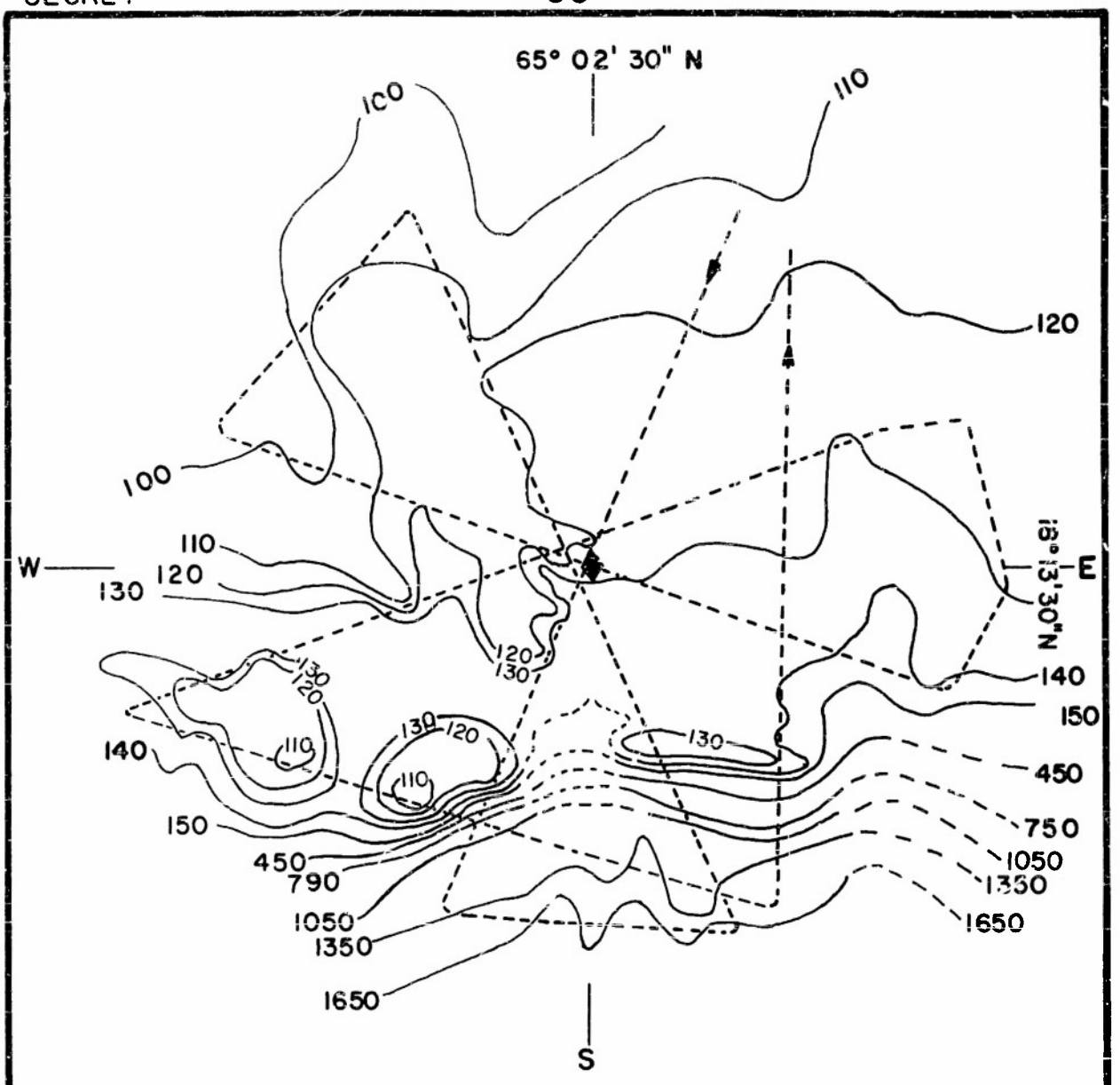


BOTTOM TOPOGRAPHY AROUND BUOY

(CONTOURS IN FEET)

---→ INDICATES SOUNDING LINES

♦ BUOY

1 0 2 4 6 8 10

SCALE IN KILOYARDS

FIG. 2

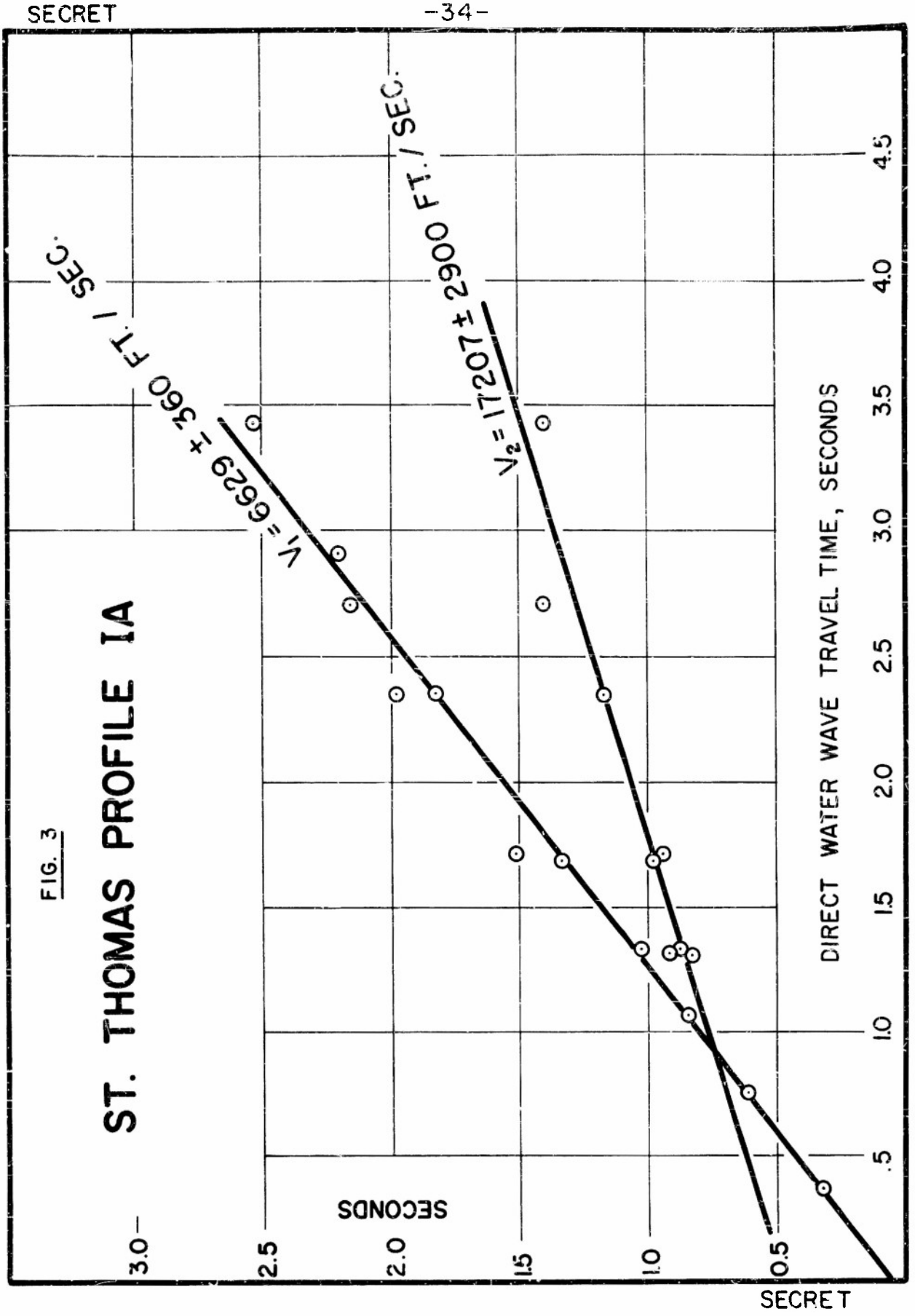
ST. THOMAS PROFILE IA
FIG. 3
$V_1 = 6629 \pm 360$ FT. / SEC.
$V_2 = 17207 \pm 2900$ FT. / SEC.
DIRECT WATER WAVE TRAVEL TIME, SECONDS
SECONDS
0.5
1.0
1.5
2.0
2.5
3.0
.5
1.0
1.5
2.0
2.5
3.0
3.5
4.0
4.5

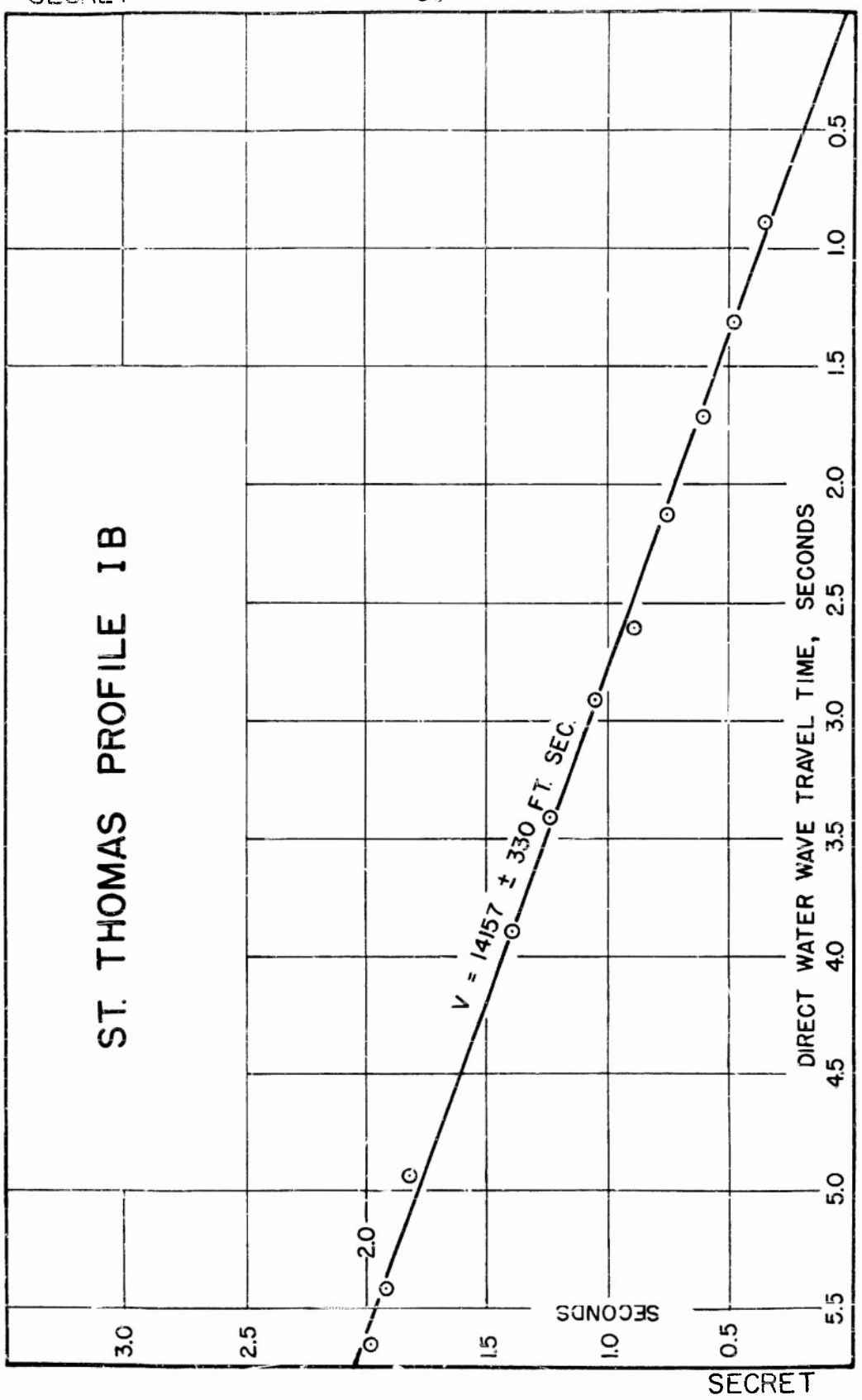
ST. THOMAS PROFILE 1B
V = 14157 ± 330 FT. SEC.
DIRECT WATER WAVE TRAVEL TIME, SECONDS
0.5
1.0
1.5
2.0
2.5
3.0
3.5
4.0
4.5
5.0
5.5
SECONDS
3.0
2.5
2.0
1.5
1.0
0.5

FIG. 4

FIG. 5

# ST. THOMAS PROFILE II A

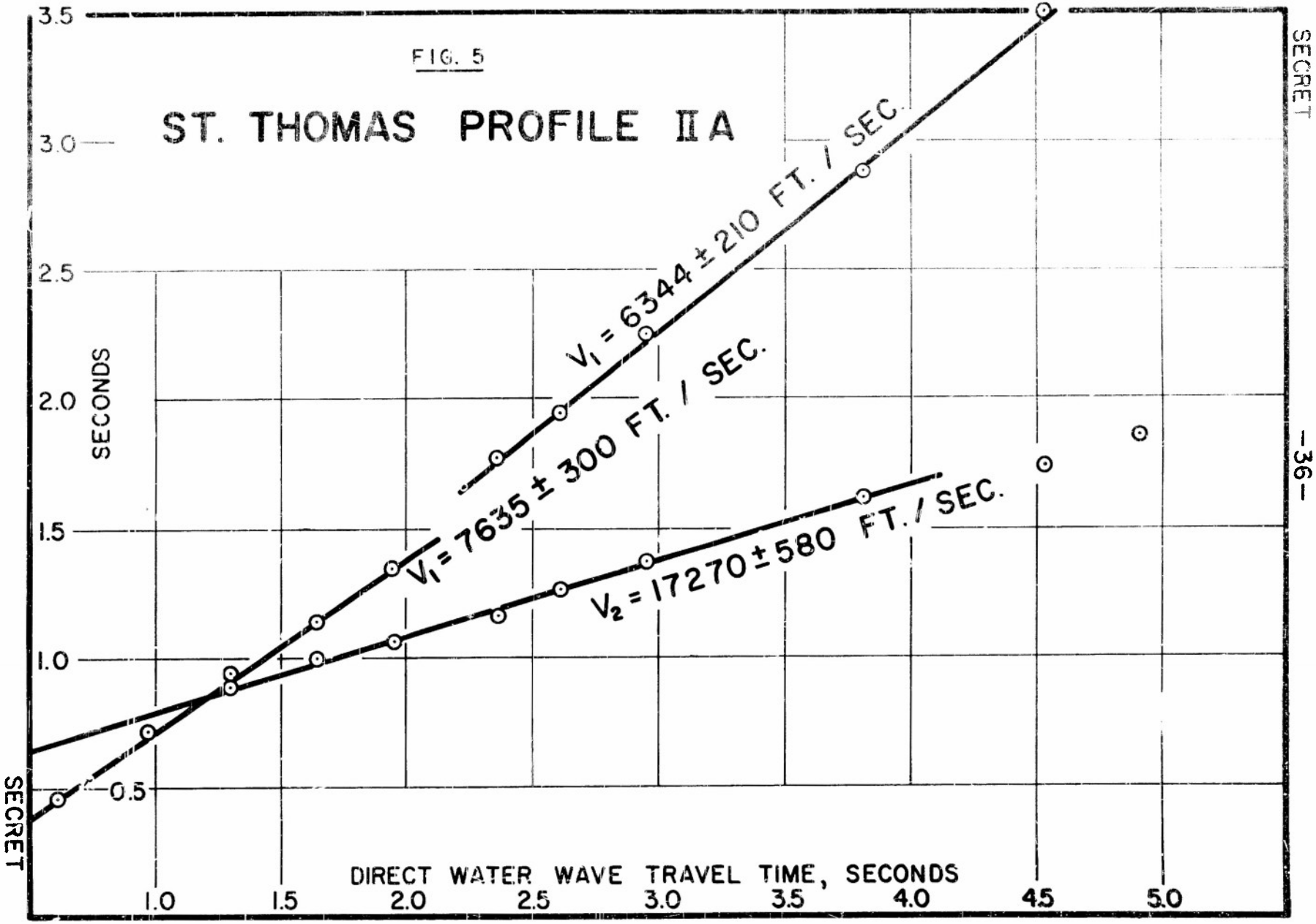

FIG. 6

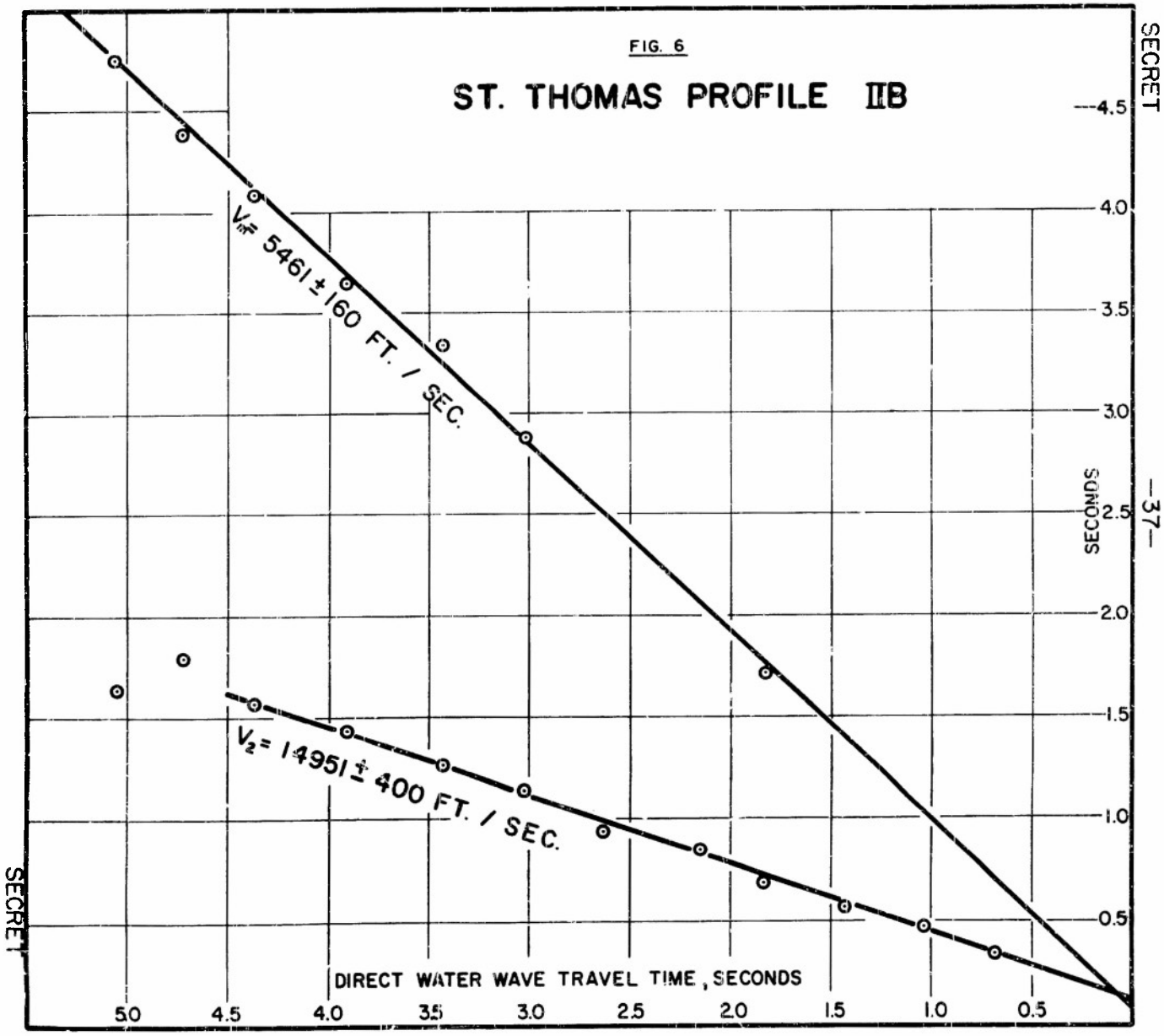
ST. THOMAS PROFILE IIB
$V_1$= 5461 ± 160 FT. / SEC.
$V_2$= 14951 ± 400 FT. / SEC.
DIRECT WATER WAVE TRAVEL TIME, SECONDS
SECONDS
5.0
4.5
4.0
3.5
3.0
2.5
2.0
1.5
1.0
0.5

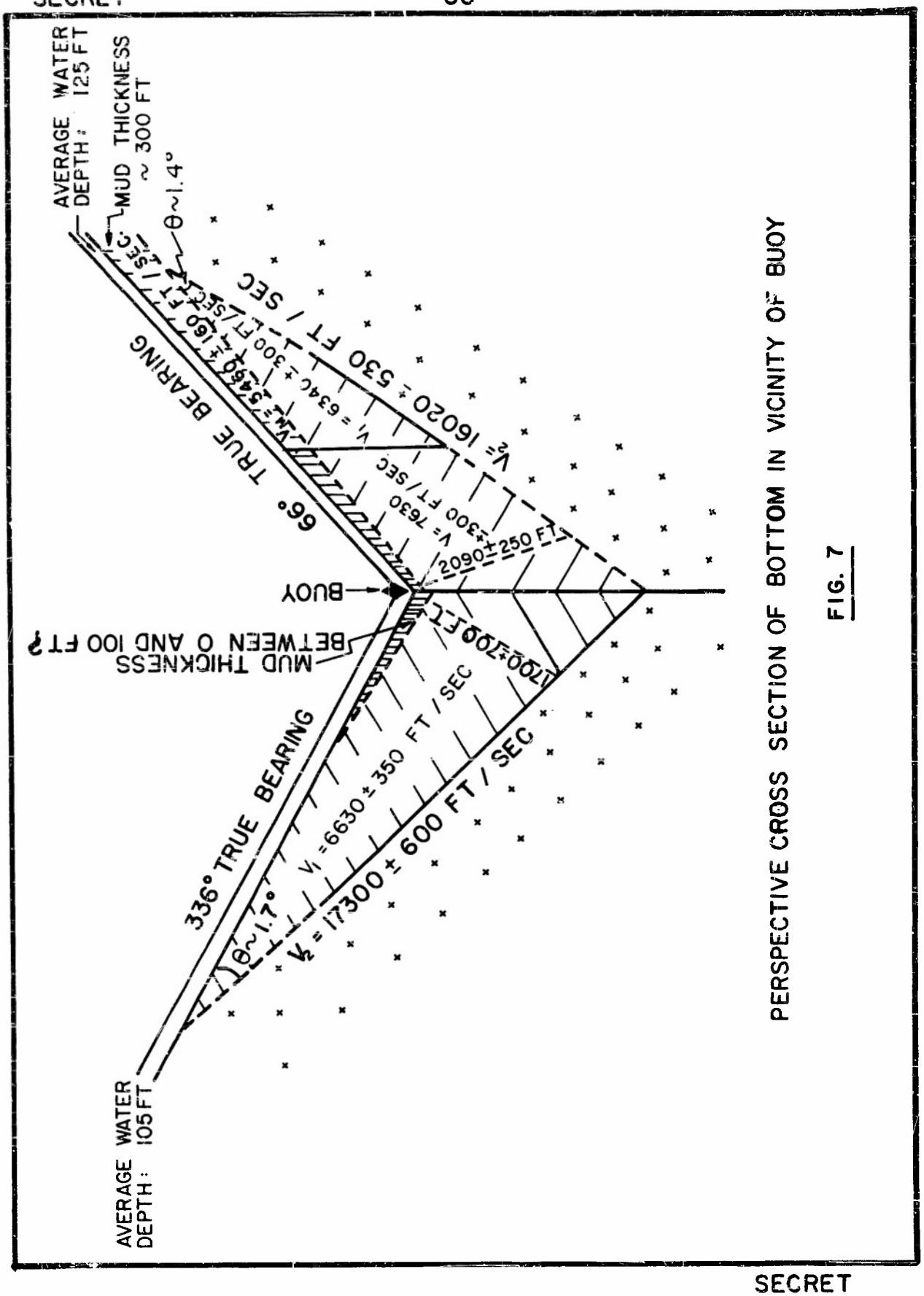


PERSPECTIVE CROSS SECTION OF BOTTOM IN VICINITY OF BUOY

FIG. 7

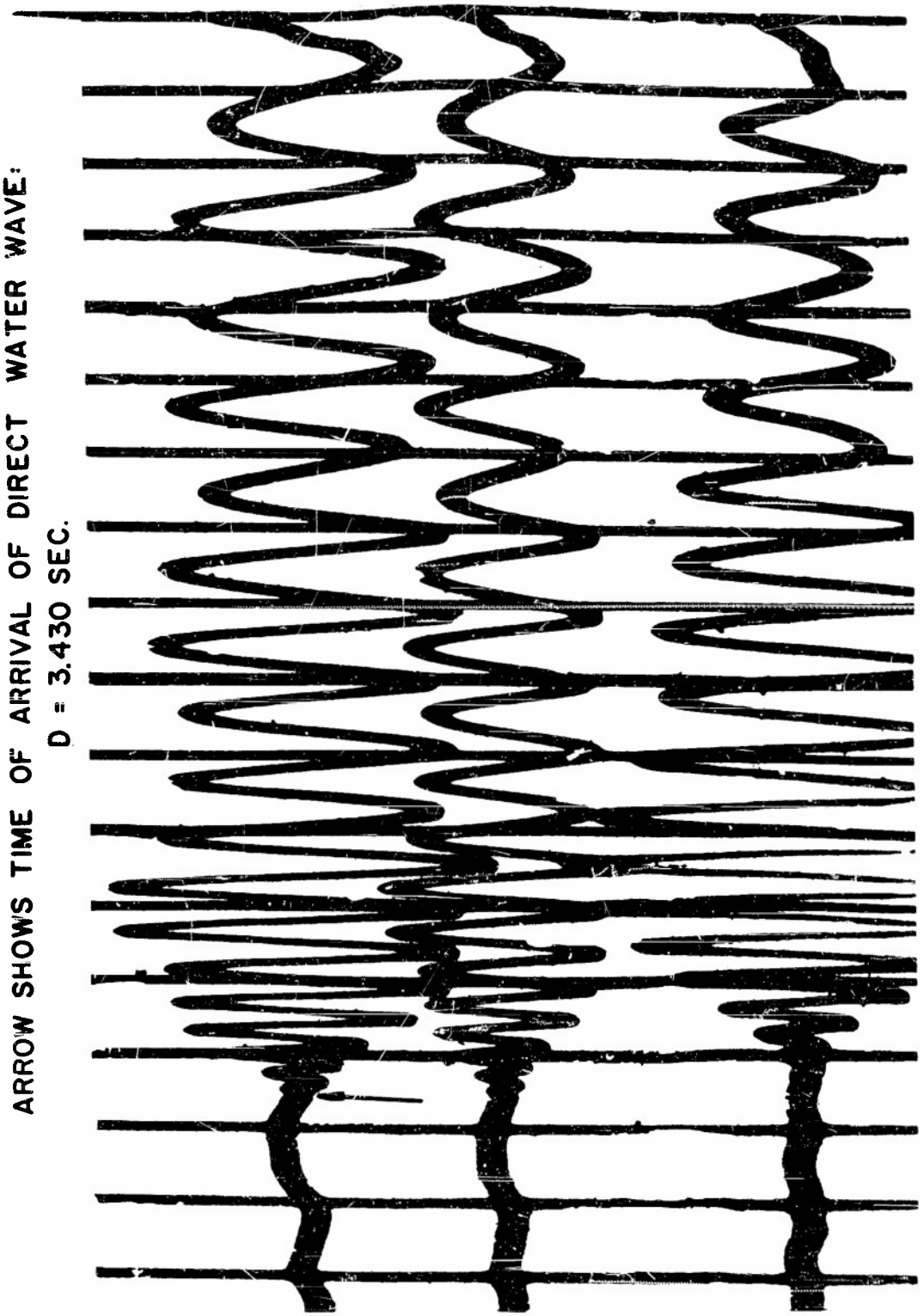

DISPERSION OF WATER WAVE TRAIN. VERTICAL LINE SPACING: 0.01 SEC.
ARROW SHOWS TIME OF ARRIVAL OF DIRECT WATER WAVE:
D = 3.430 SEC.

FIG. 8

# FIG. 9

## GROUP VELOCITY VS FREQUENCY POINTS SHOT DATA

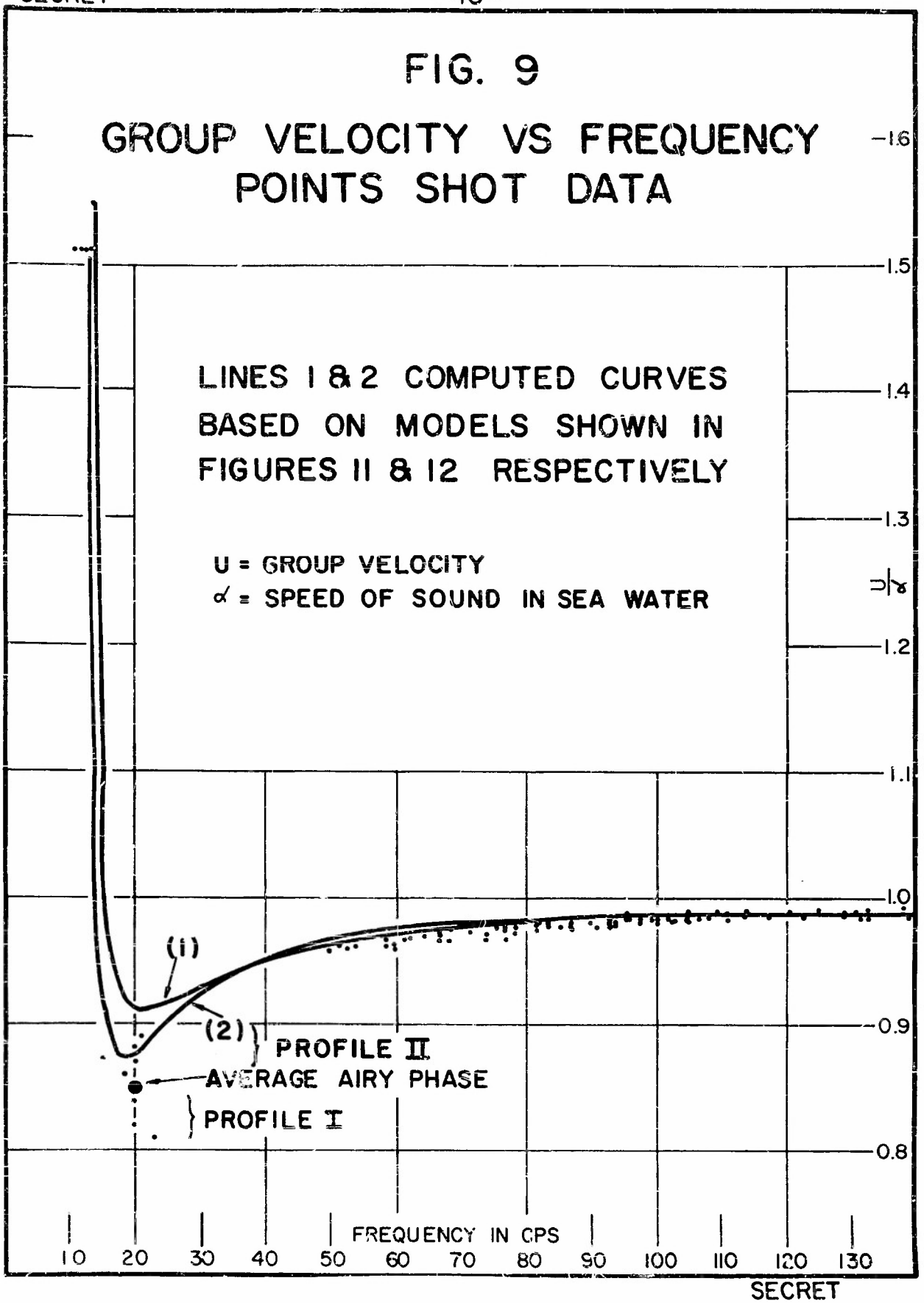

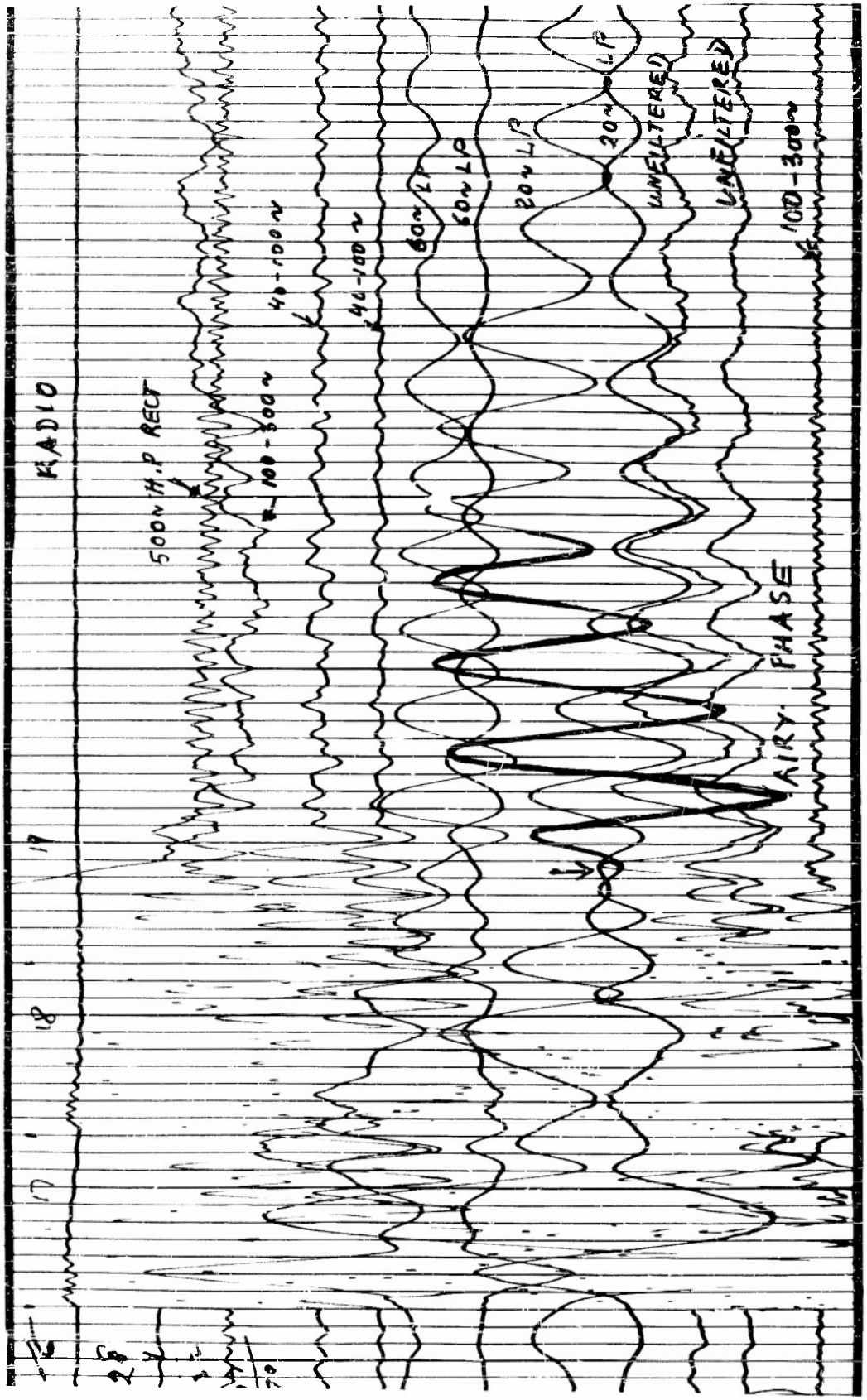


FIG. 10

AIRY PHASE OF SHOT #3, PROFILE I B

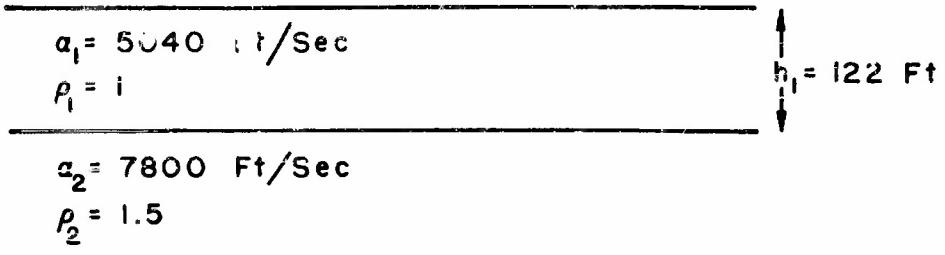


FIG. 11

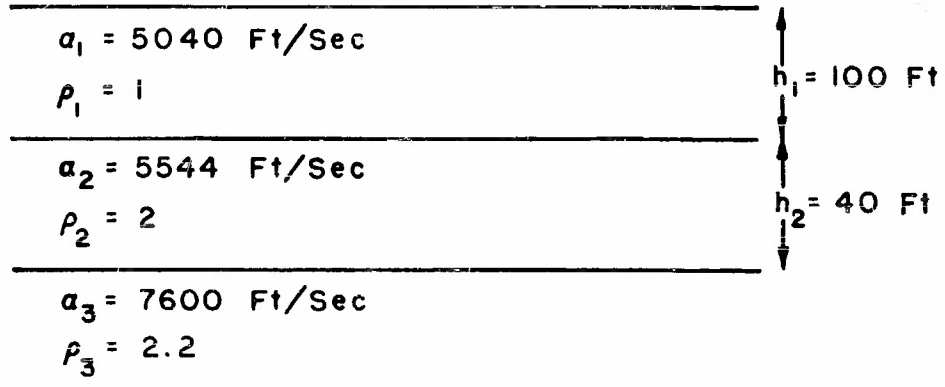


FIG. 12

MODELS USED FOR COMPUTATION OF DISPERSION CURVES SHOWN IN FIG. 9.

# BLOCK DIAGRAM OF RECORDING EQUIPMENT

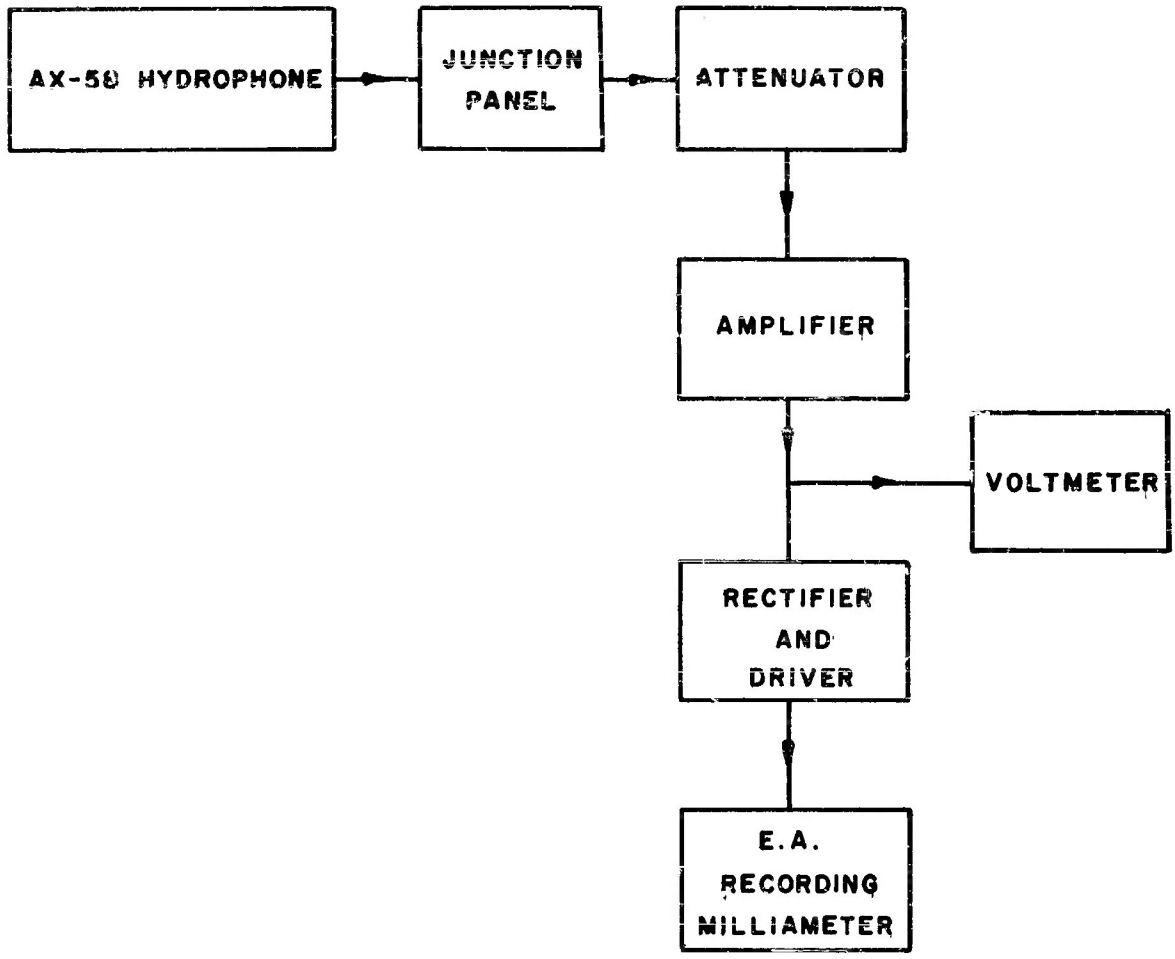


FIG. 13

FIG. 14

# AMPLIFIER GAIN

THE DISCONTINUITY AT 15 CPS CORRESPONDS TO THE OVERLAP OF THE 5-15 AND 15-40 CPS RANGES GIVEN BY A RANGE SELECTOR SWITCH

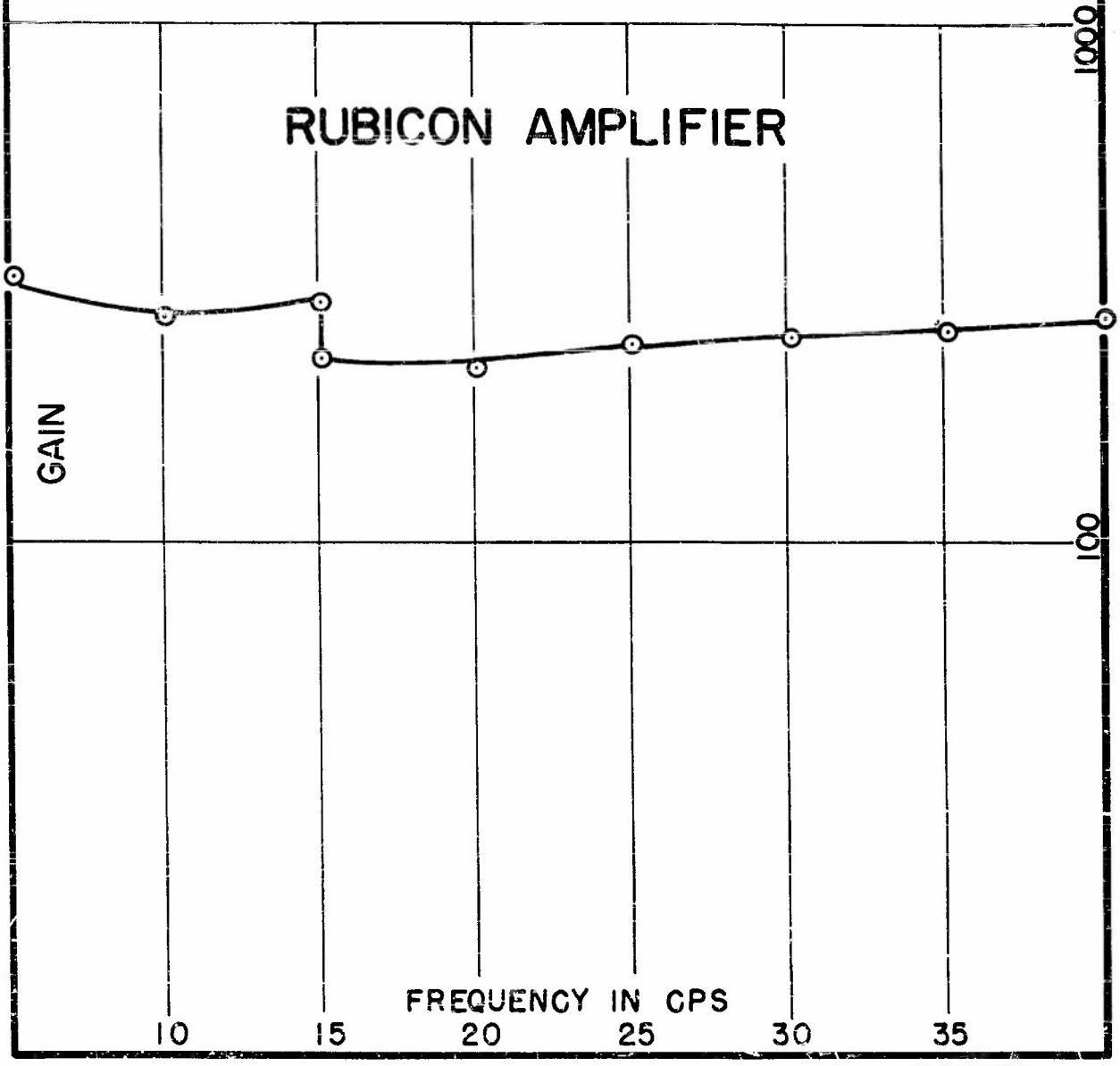

FIG. 15

# HYDROPHONE SENSITIVITIES

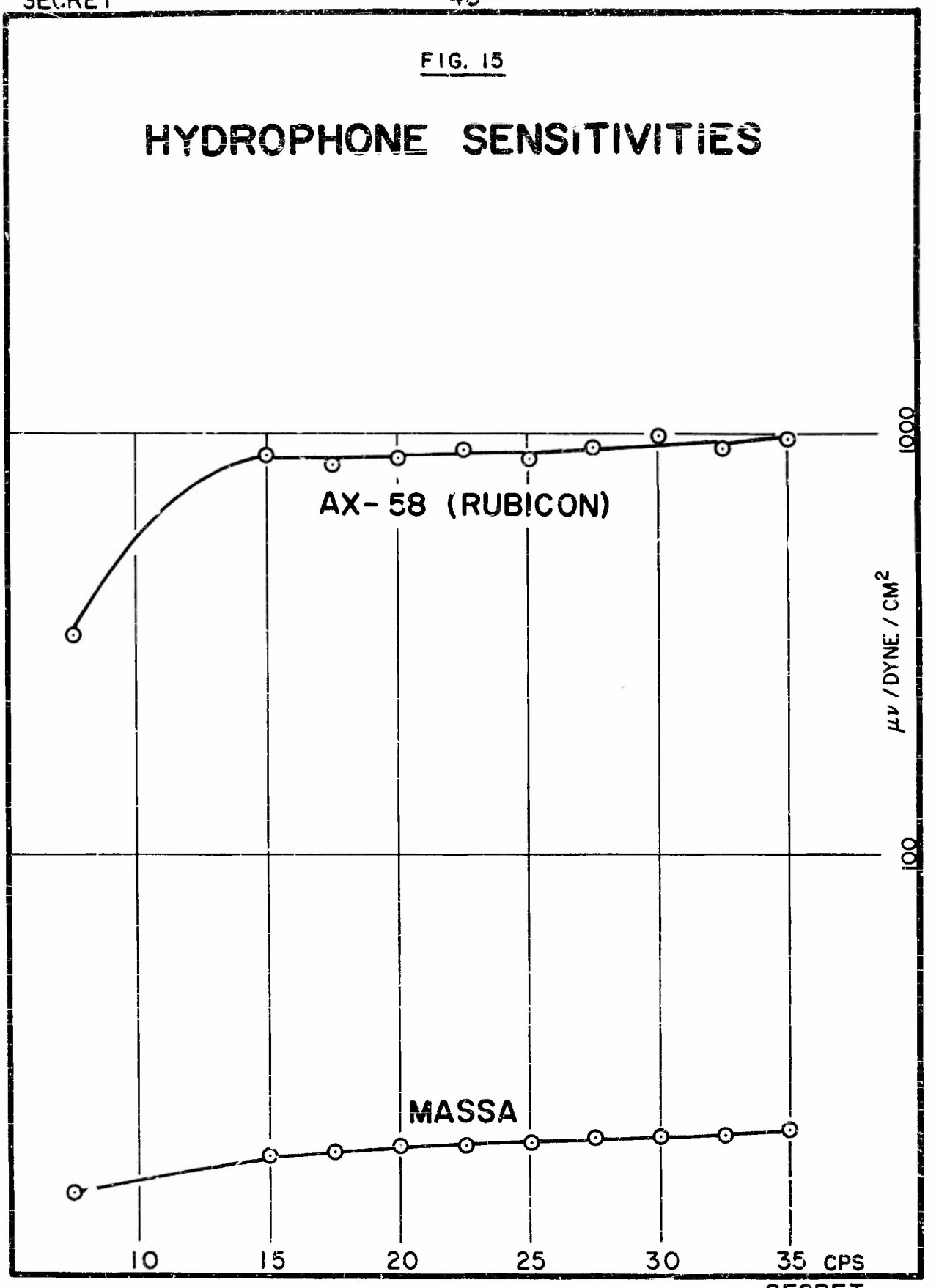

# FIG. 16

# SYSTEM FOR HYDROPHONE TOWING

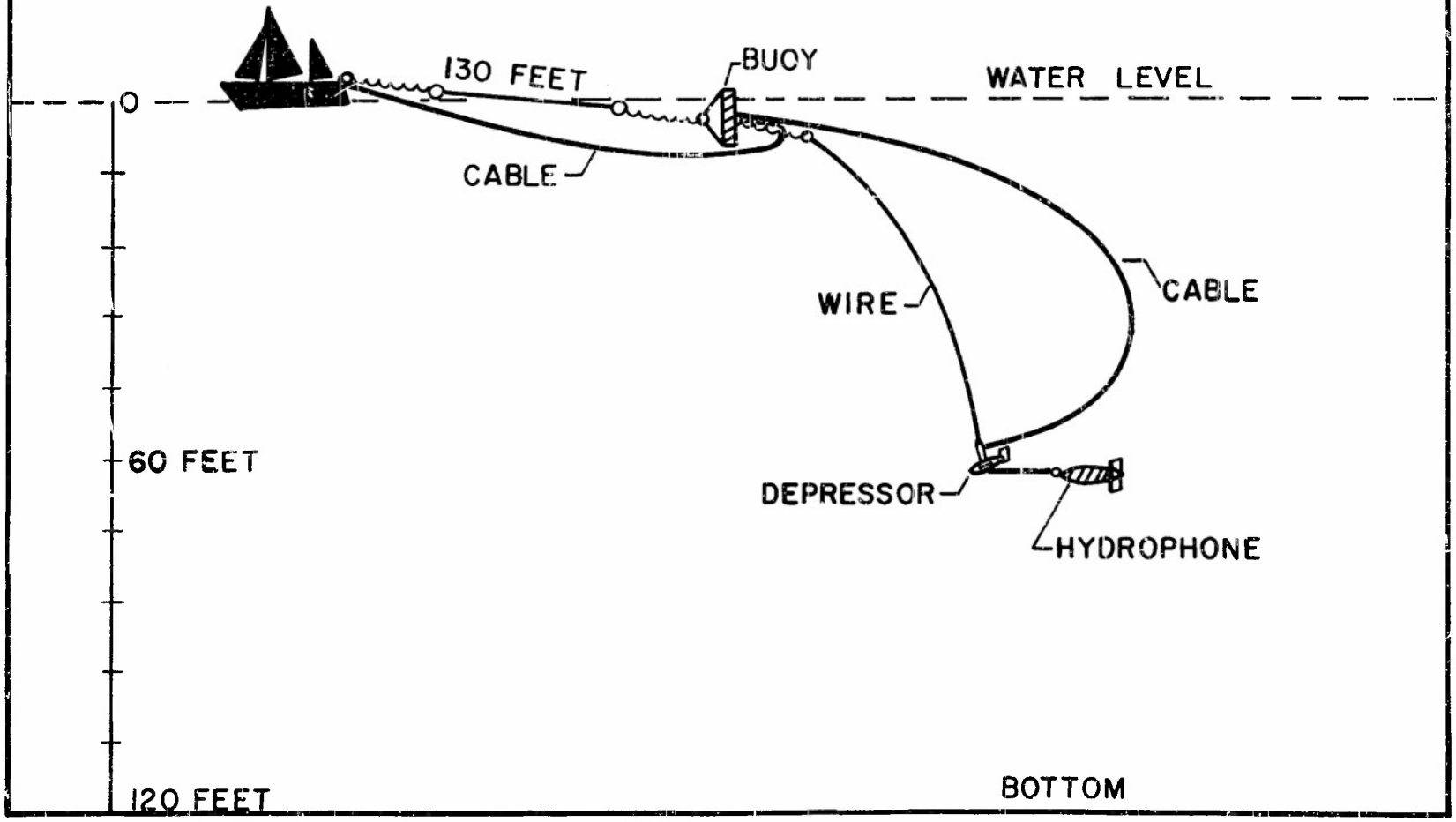

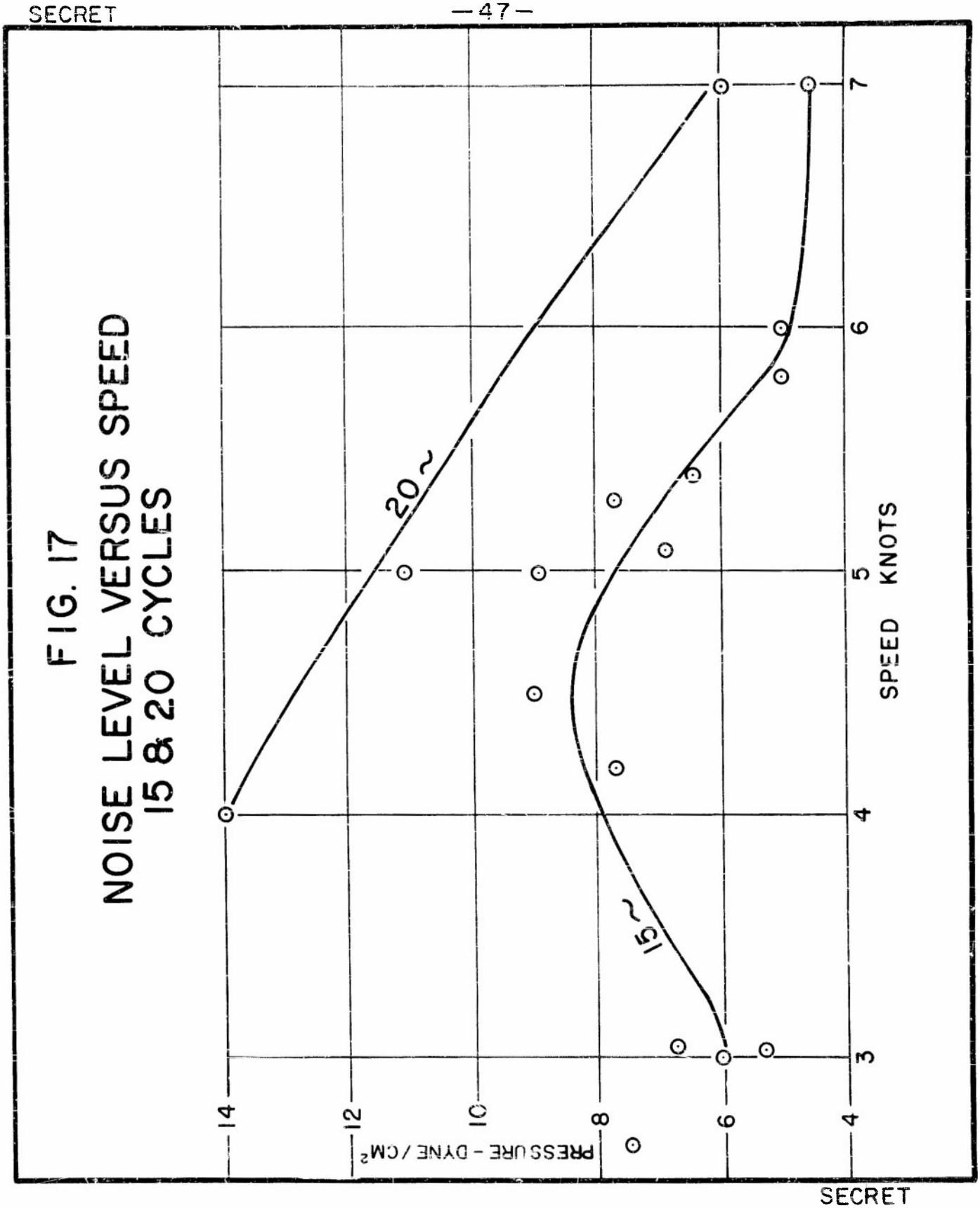
FIG. 17
NOISE LEVEL VERSUS SPEED
15 & 20 CYCLES
20~
15~
PRESSURE - DYNE / CM²
14
12
10
8
6
4
3
4
5
6
7
SPEED KNOTS

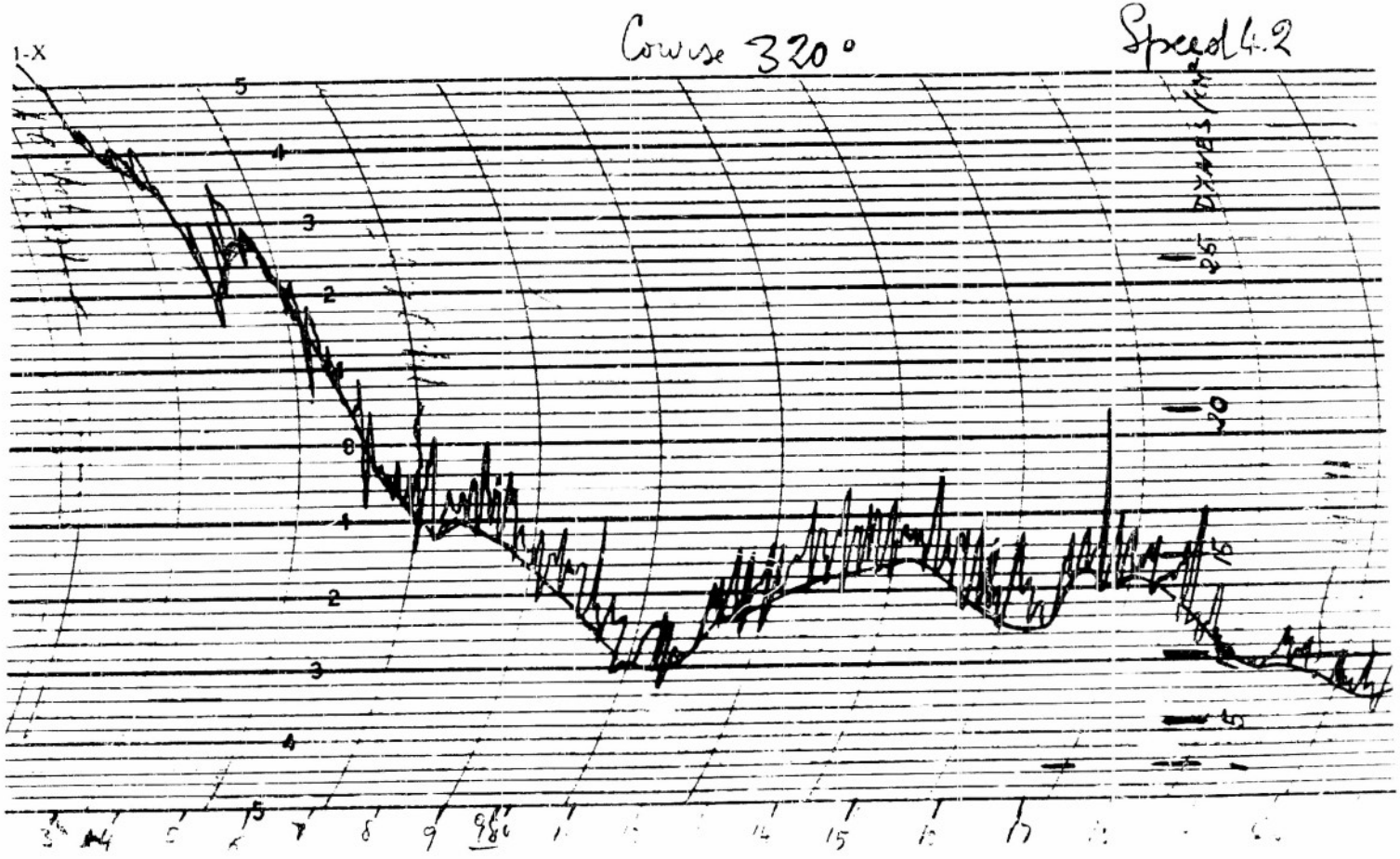


FIG. 18

A TYPICAL 15 CPS ESTERLINE-ANGUS RECORDING OF PRESSURE FIELD.
THE SCALE IN DYNES / CM² IS SHOWN TO THE RIGHT

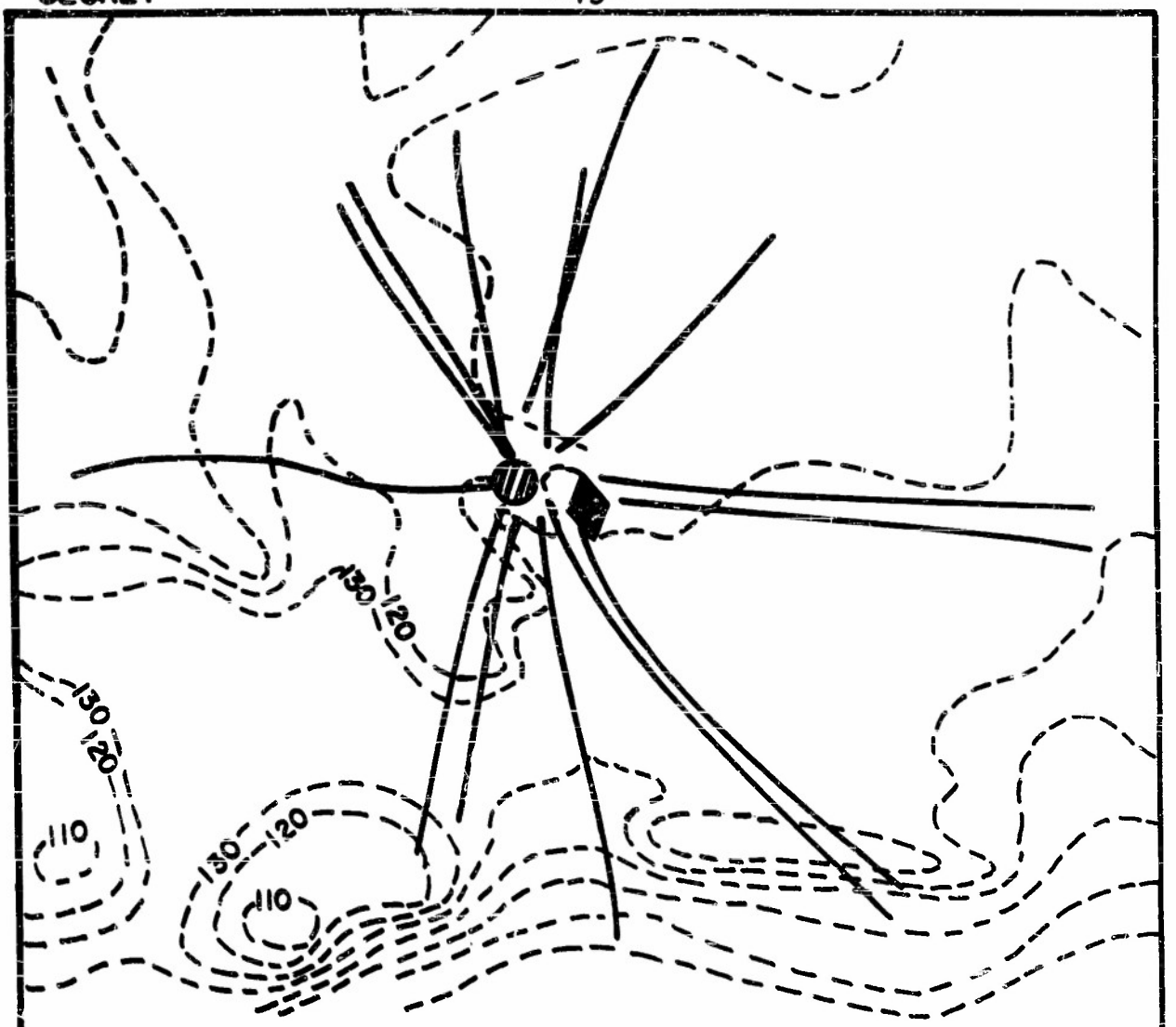


FIG. 19

THE POSITION OF THE SOURCE THROUGHOUT ALL THE RUNS (SOLID LINES) WAS INSIDE OF THE CIRCLE W OF THE BUOY

PRESSURE FIELD SURVEY RUNS AT 20 CPS

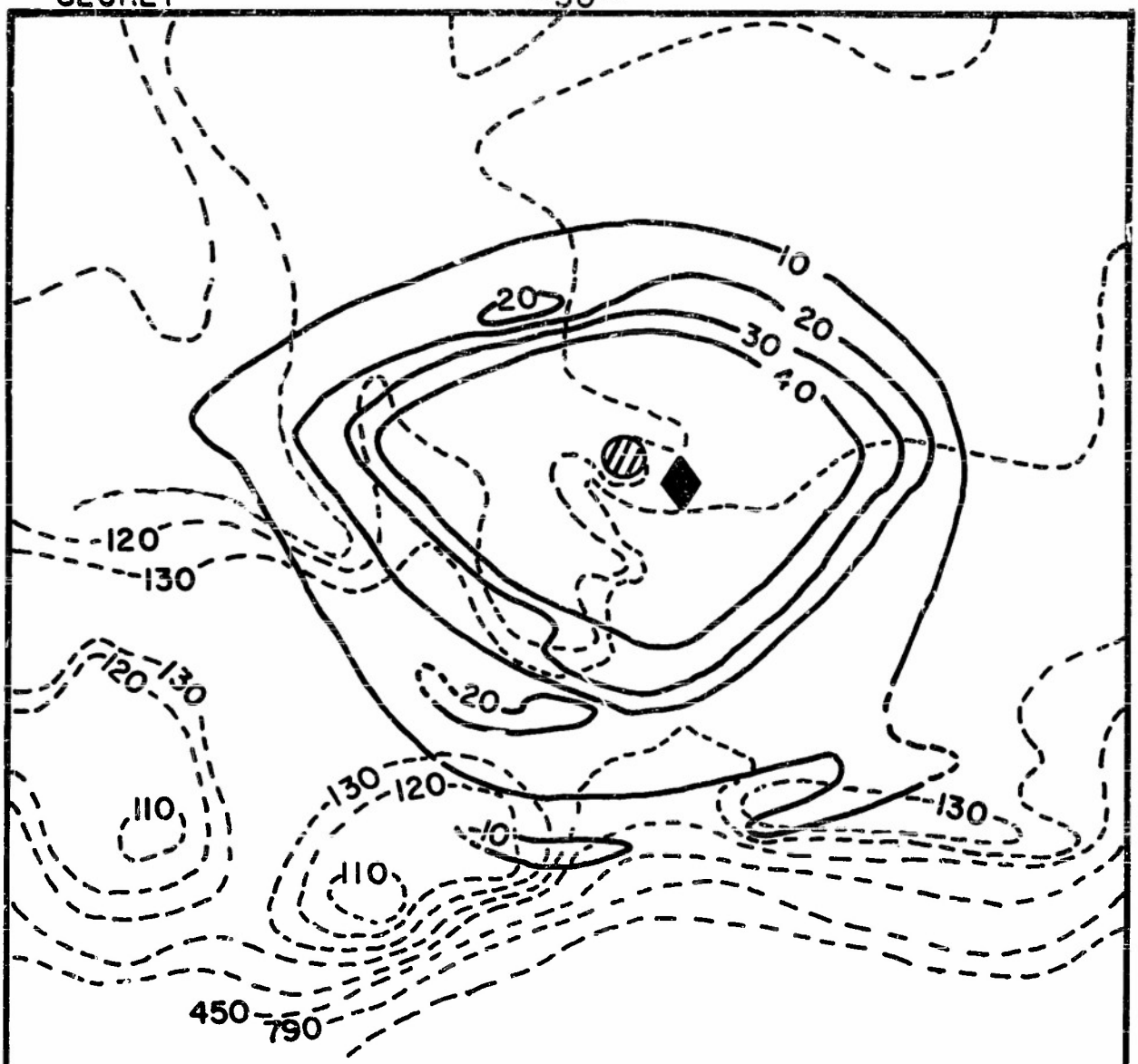


FIG. 20

SOLID CONTOURS: PRESSURE FIELD R.M.S. AMPLITUDE IN DYNES/CM$^2$

DOTTED CONTOURS: WATER DEPTH IN FEET

PRESSURE FIELD AT 20 CPS

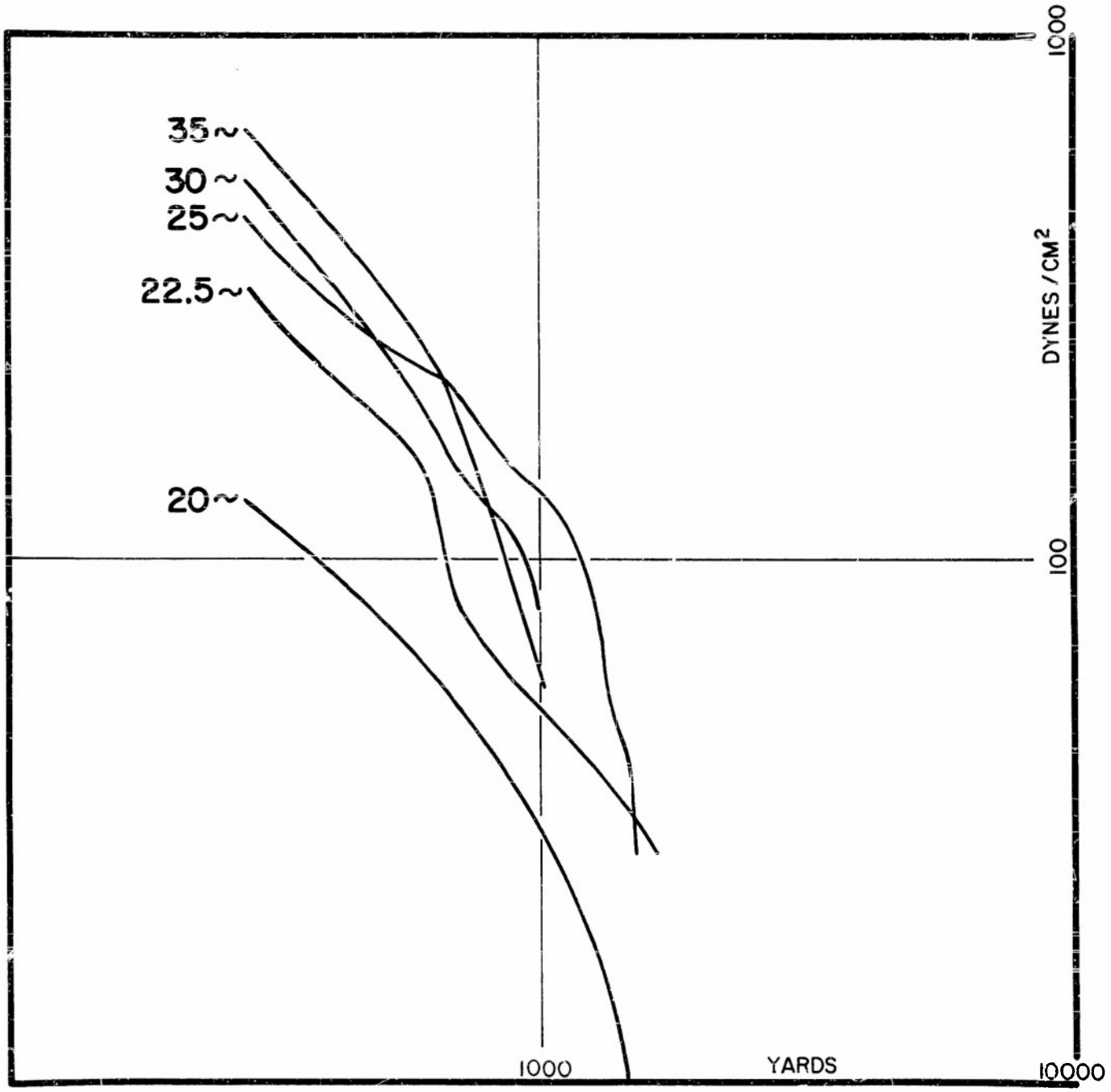


COMPARISON OF PRESSURE VS RANGE CURVES ALONG NEIGHBORING TRACKS FOR DIFFERENT FREQUENCIES

FIG. 21

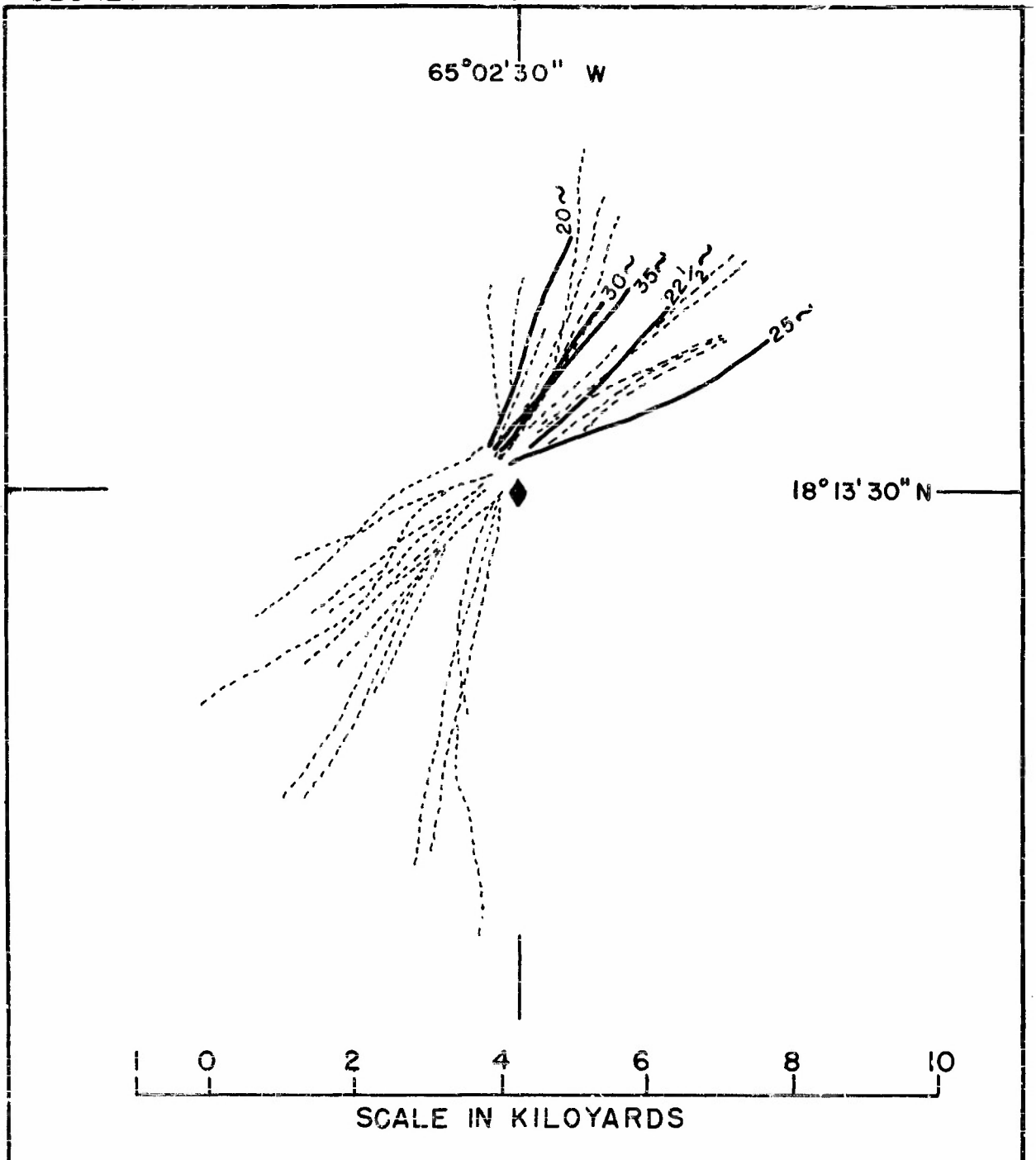


FIG. 22

RUNS UTILIZED IN FIGS. 21 AND 35 (SOLID LINES) AND FIGS. 23, 24, 25 (SOLID AND DOTTED LINES)

FIG. 23

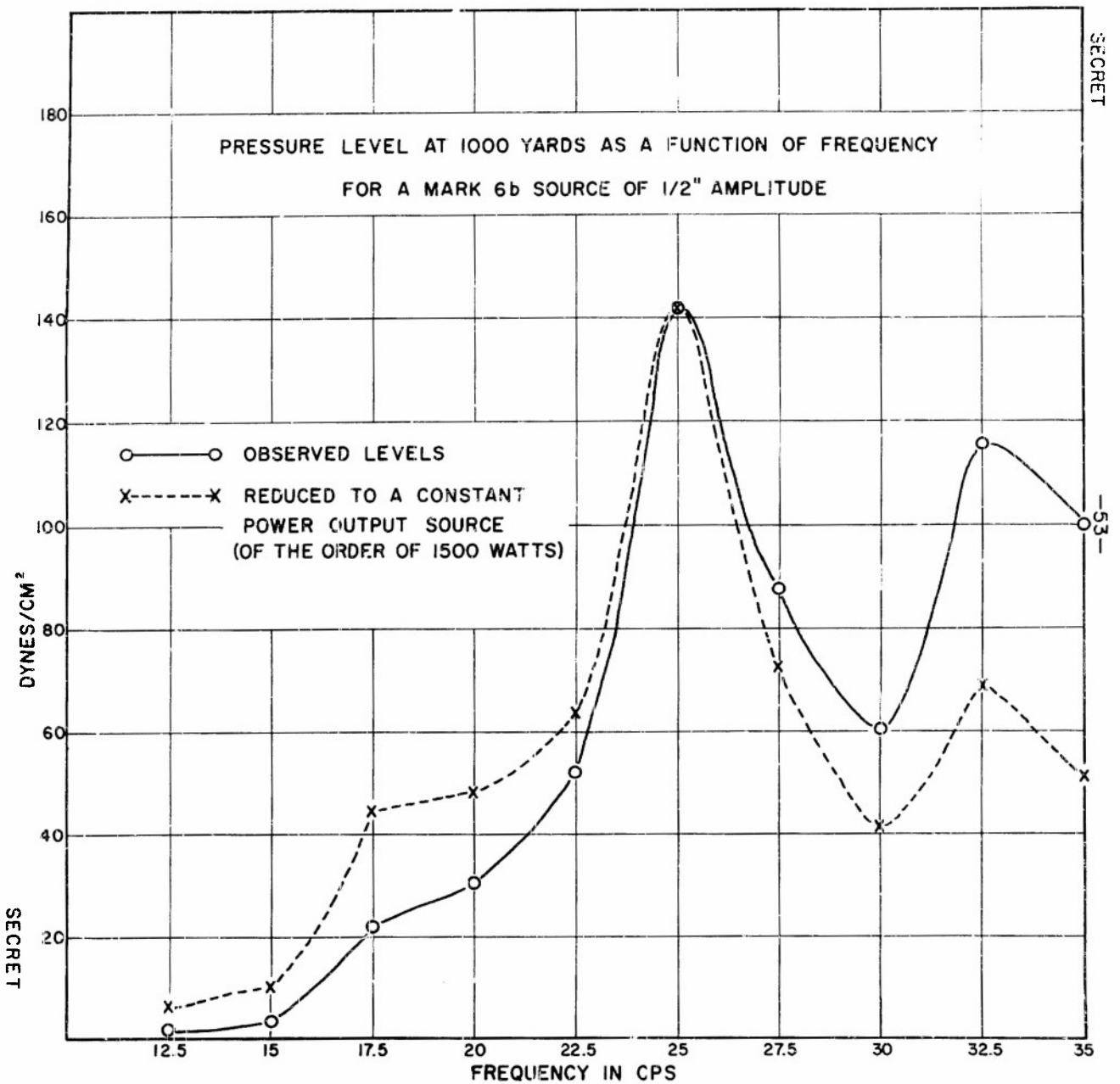
SECRET
PRESSURE LEVEL AT 1000 YARDS AS A FUNCTION OF FREQUENCY
FOR A MARK 6b SOURCE OF 1/2" AMPLITUDE
OBSERVED LEVELS
REDUCED TO A CONSTANT POWER OUTPUT SOURCE (OF THE ORDER OF 1500 WATTS)
DYNES/CM²
180
160
140
120
100
80
60
40
20
12.5
15
17.5
20
22.5
25
27.5
30
32.5
35
FREQUENCY IN CPS
SECRET

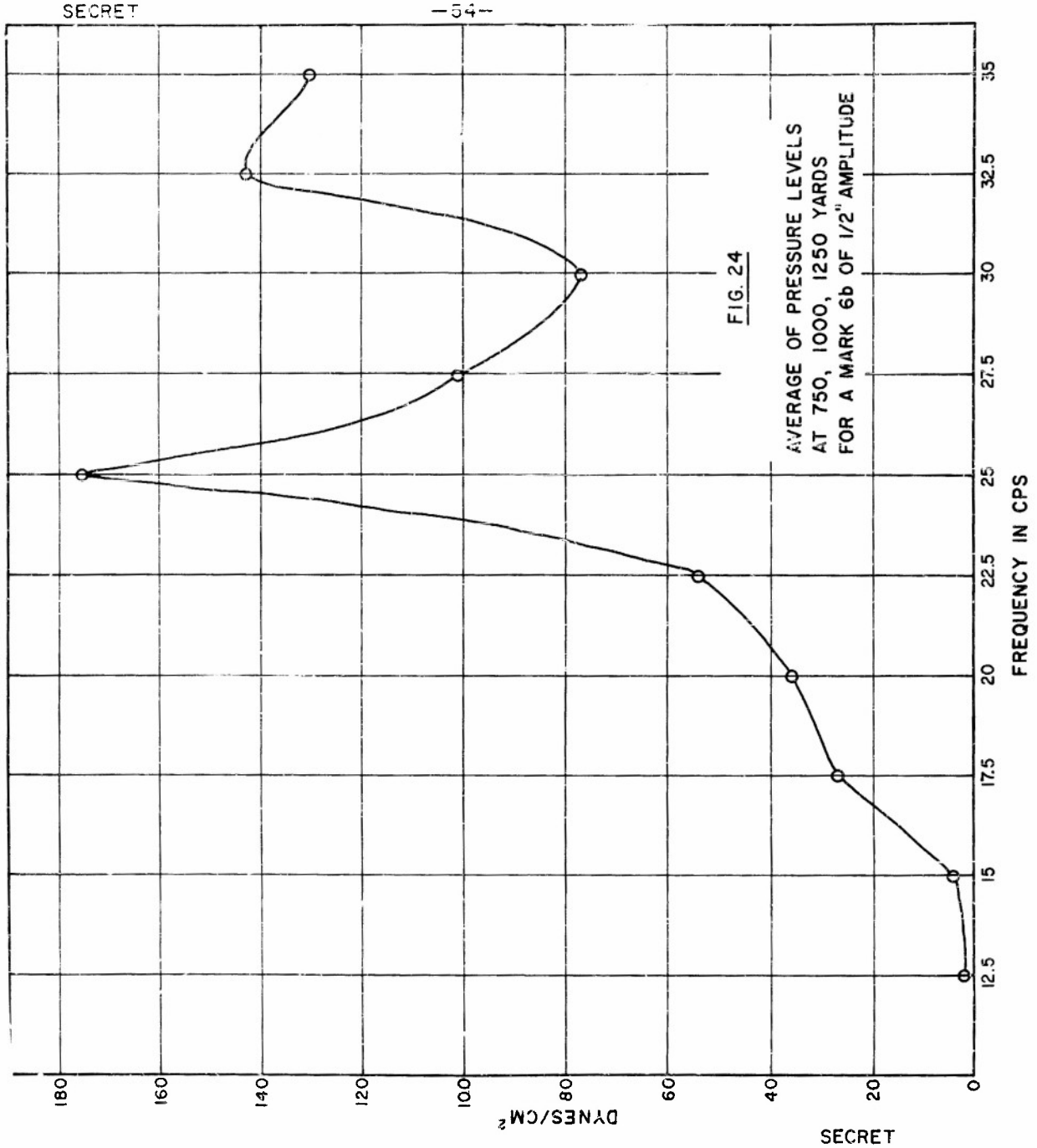
AVERAGE OF PRESSURE LEVELS
AT 750, 1000, 1250 YARDS
FOR A MARK 6b OF 1/2" AMPLITUDE
DYNES/CM²
0
20
40
60
80
100
120
140
160
180
12.5
15
17.5
20
22.5
25
27.5
30
32.5
35
FREQUENCY IN CPS

FIG. 24

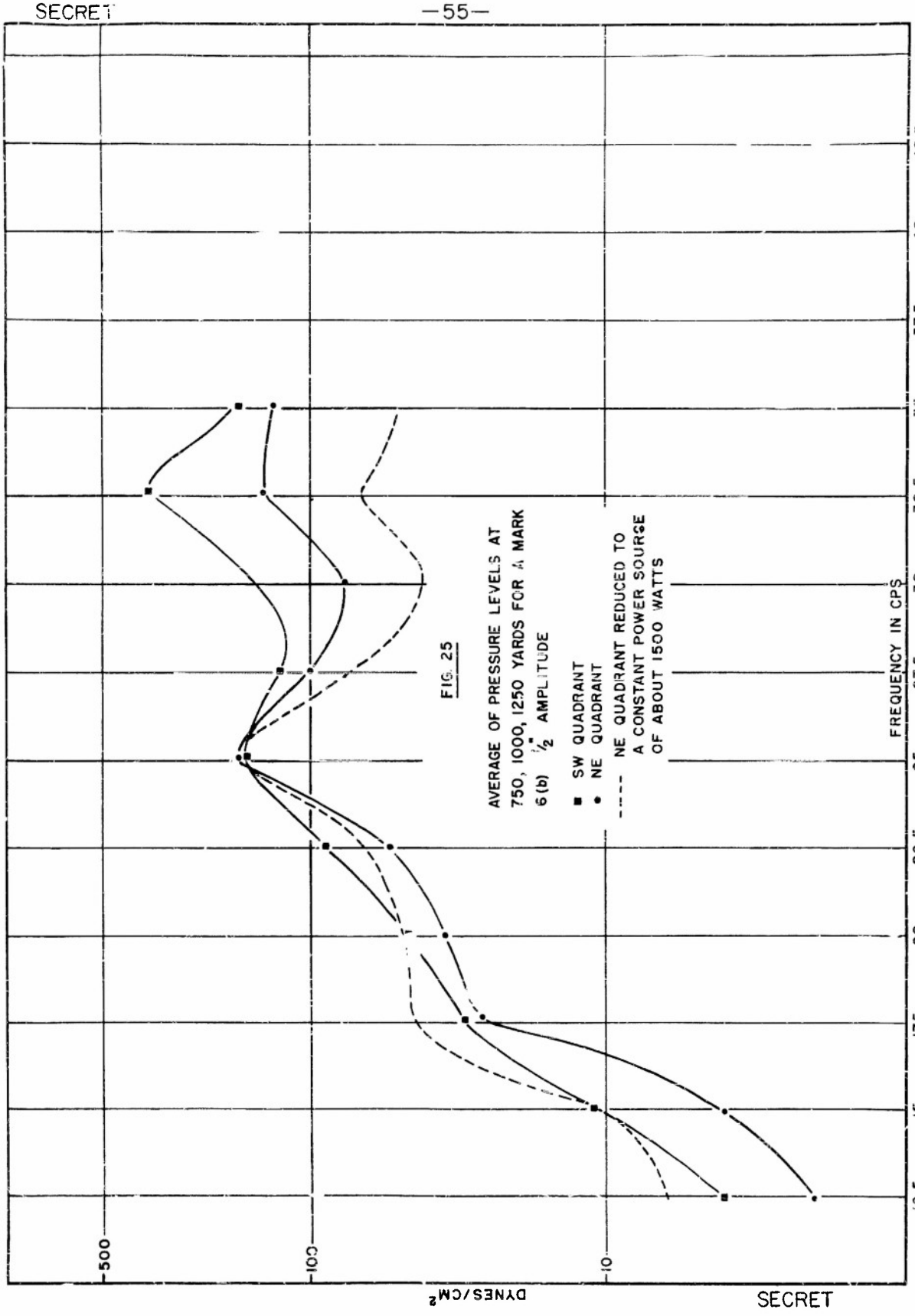
FIG. 25
AVERAGE OF PRESSURE LEVELS AT
750, 1000, 1250 YARDS FOR A MARK
6 (b) ½" AMPLITUDE
■ SW QUADRANT
• NE QUADRANT
---- NE QUADRANT REDUCED TO
A CONSTANT POWER SOURCE
OF ABOUT 1500 WATTS
500
100
10
DYNES/CM²
12.5
15
17.5
20
22.5
25
27.5
30
32.5
35
37.5
40
42.5
45
FREQUENCY IN CPS

FIG. 26

PRESSURE AMPLITUDE VS RANGE, 12.5 CPS
CORRESPONDING TO RUN SHOWN IN FIG. 34
A MARK 6(b) 1/2" AMPLITUDE

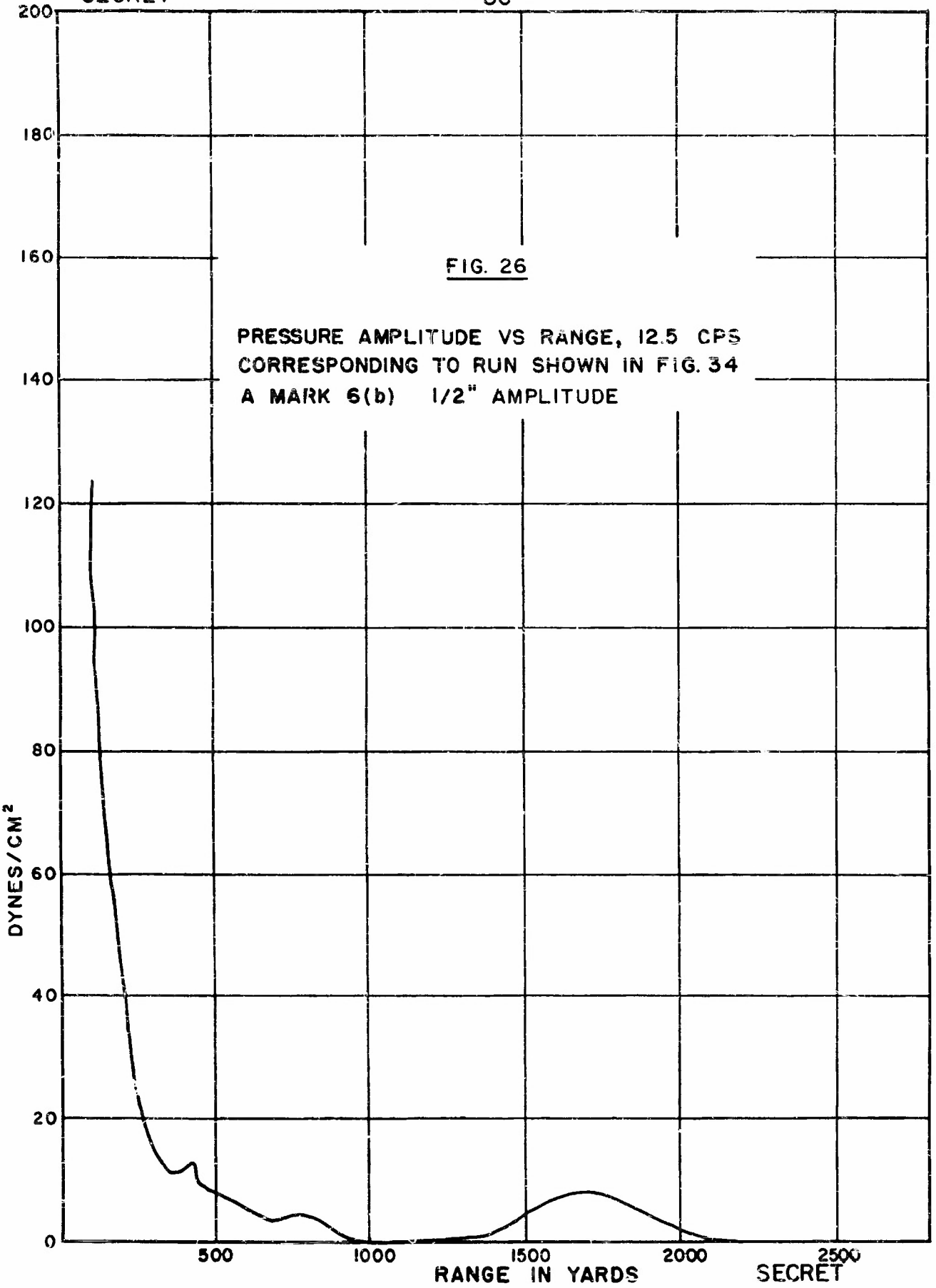

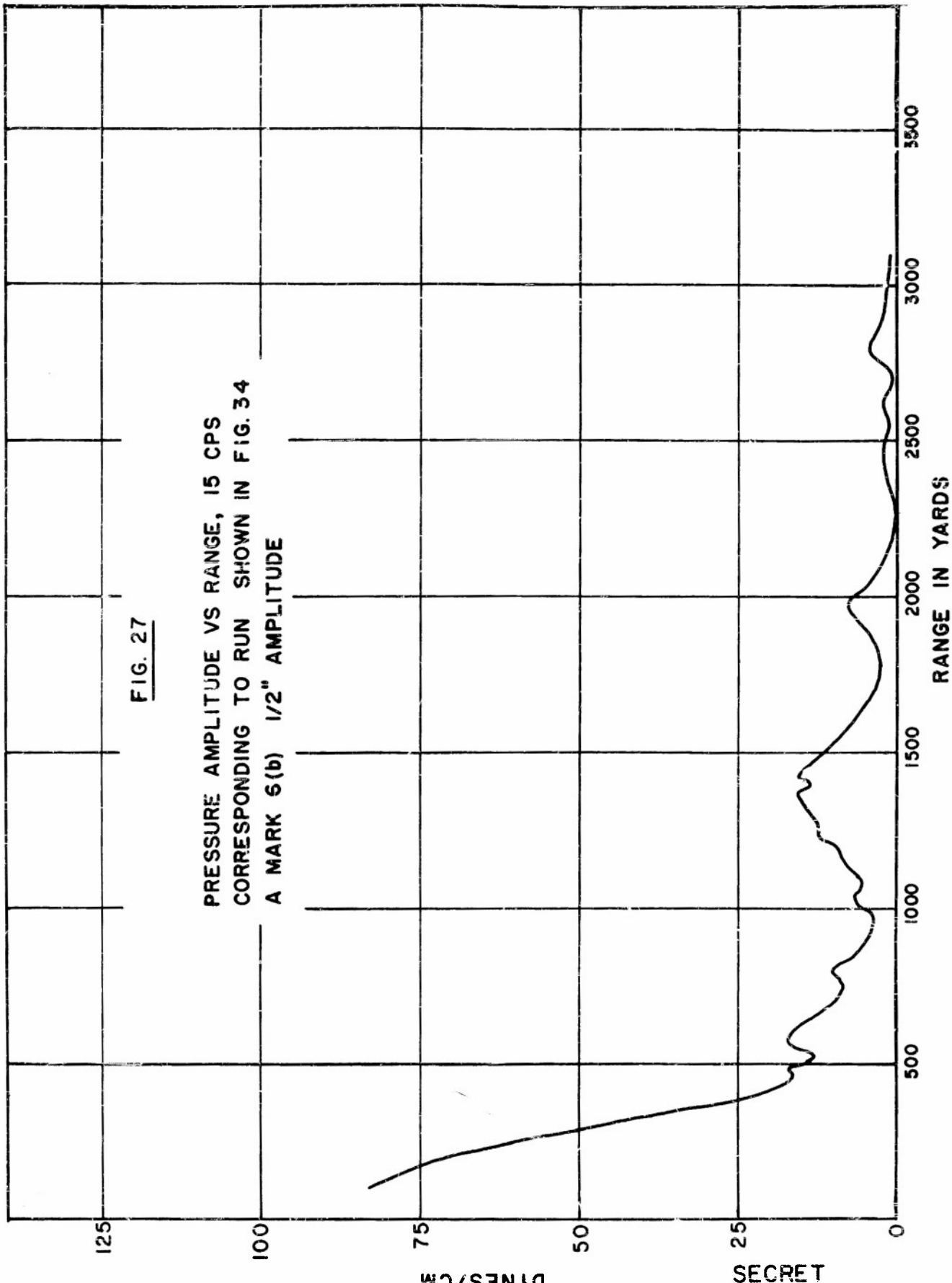
PRESSURE AMPLITUDE VS RANGE, 15 CPS
CORRESPONDING TO RUN SHOWN IN FIG. 34
A MARK 6(b) 1/2" AMPLITUDE
DYNES/CM²
0
25
50
75
100
125
500
1000
1500
2000
2500
3000
3500
RANGE IN YARDS

FIG. 27

FIG. 28

PRESSURE AMPLITUDE VS RANGE, 20 CPS
CORRESPONDING TO 20 CPS RUN INDICATED
BY (1) IN FIGS. 34 AND 36
(A MARK 6(b) 1/2" AMPLITUDE)

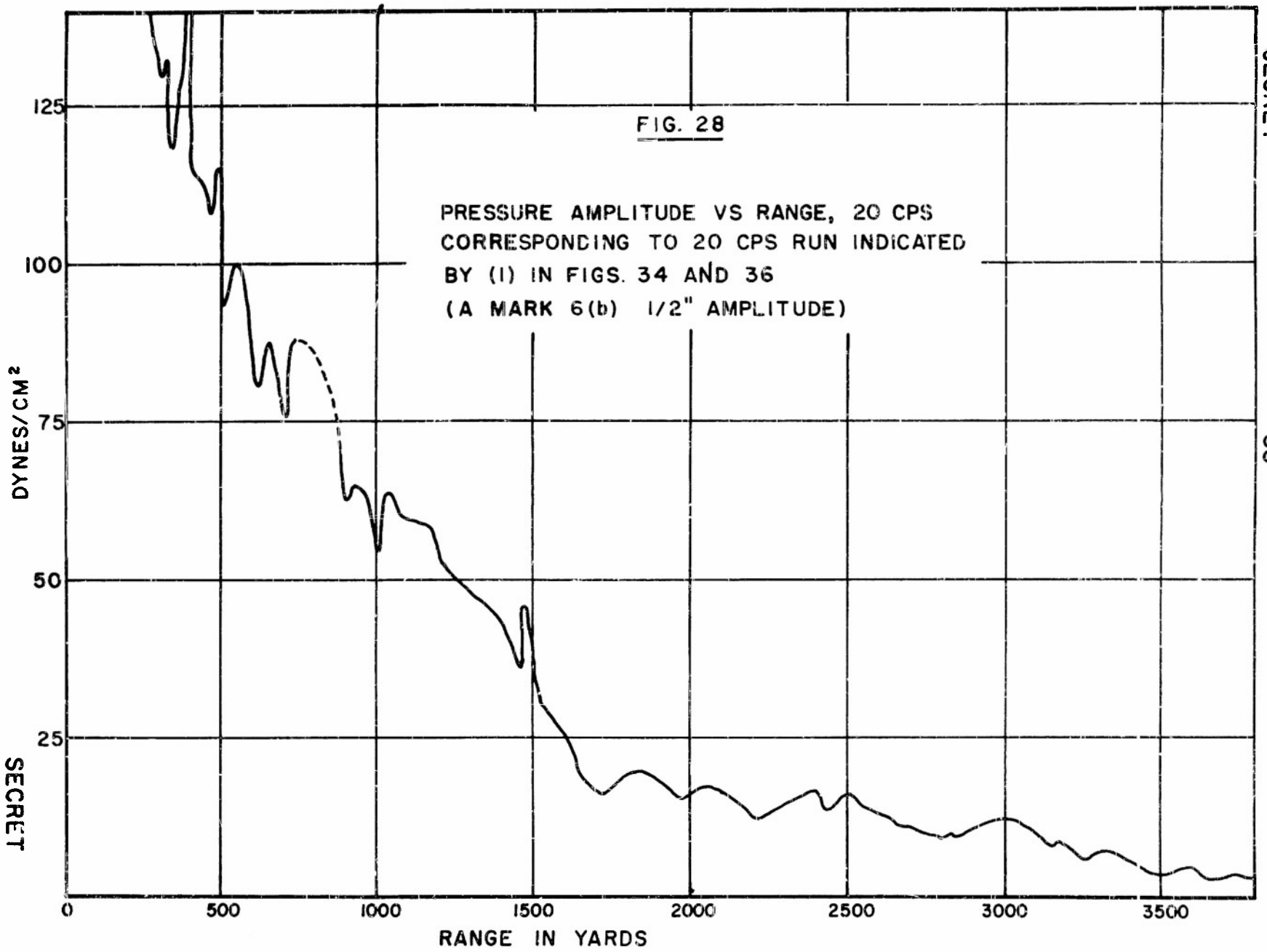

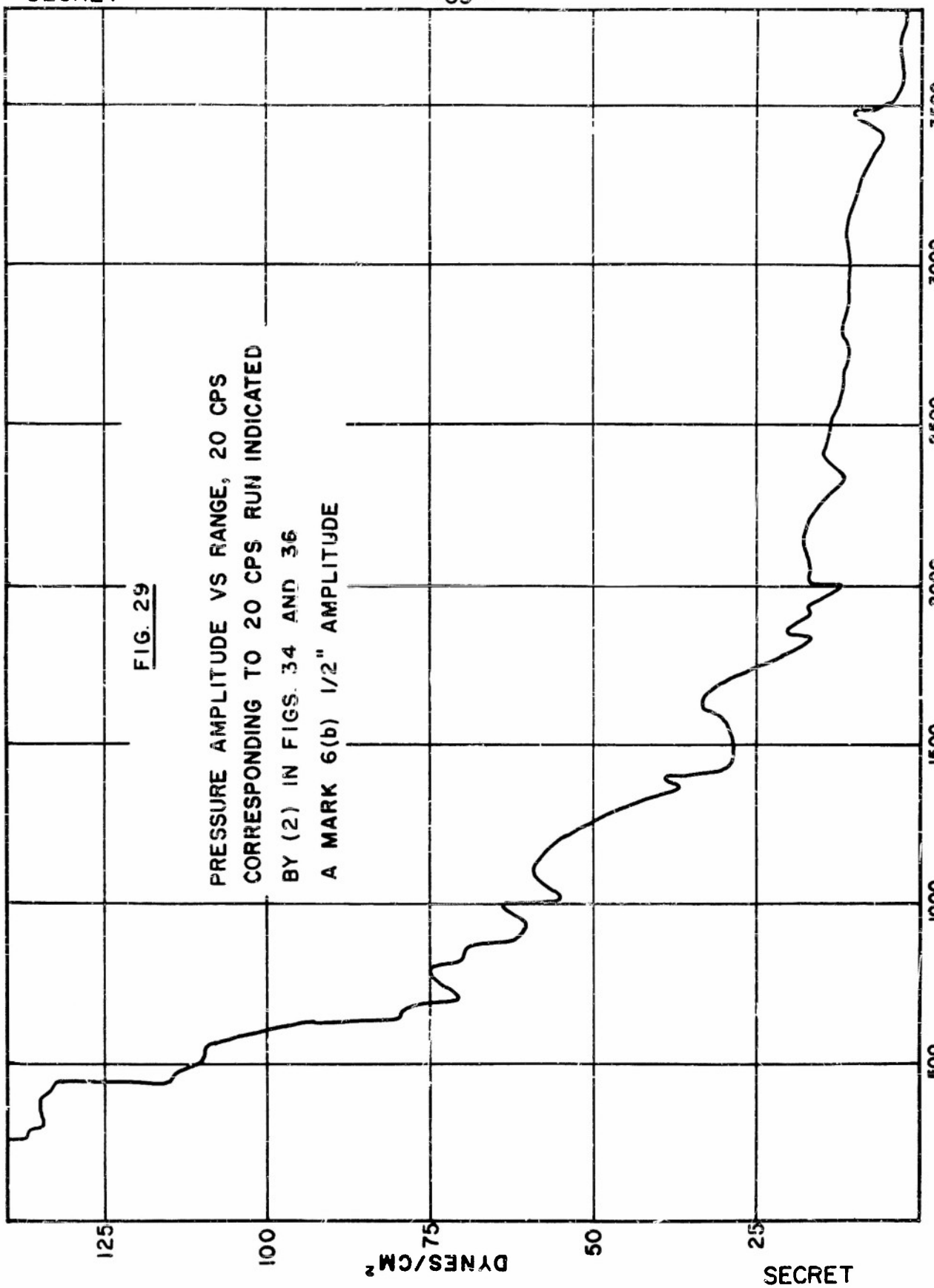
PRESSURE AMPLITUDE VS RANGE, 20 CPS
CORRESPONDING TO 20 CPS RUN INDICATED
BY (2) IN FIGS. 34 AND 36
A MARK 6(b) 1/2" AMPLITUDE
125
100
75
50
25
DYNES/CM²
500
1000
1500
2000
2500
3000
3500
RANGE IN YARDS

FIG. 29

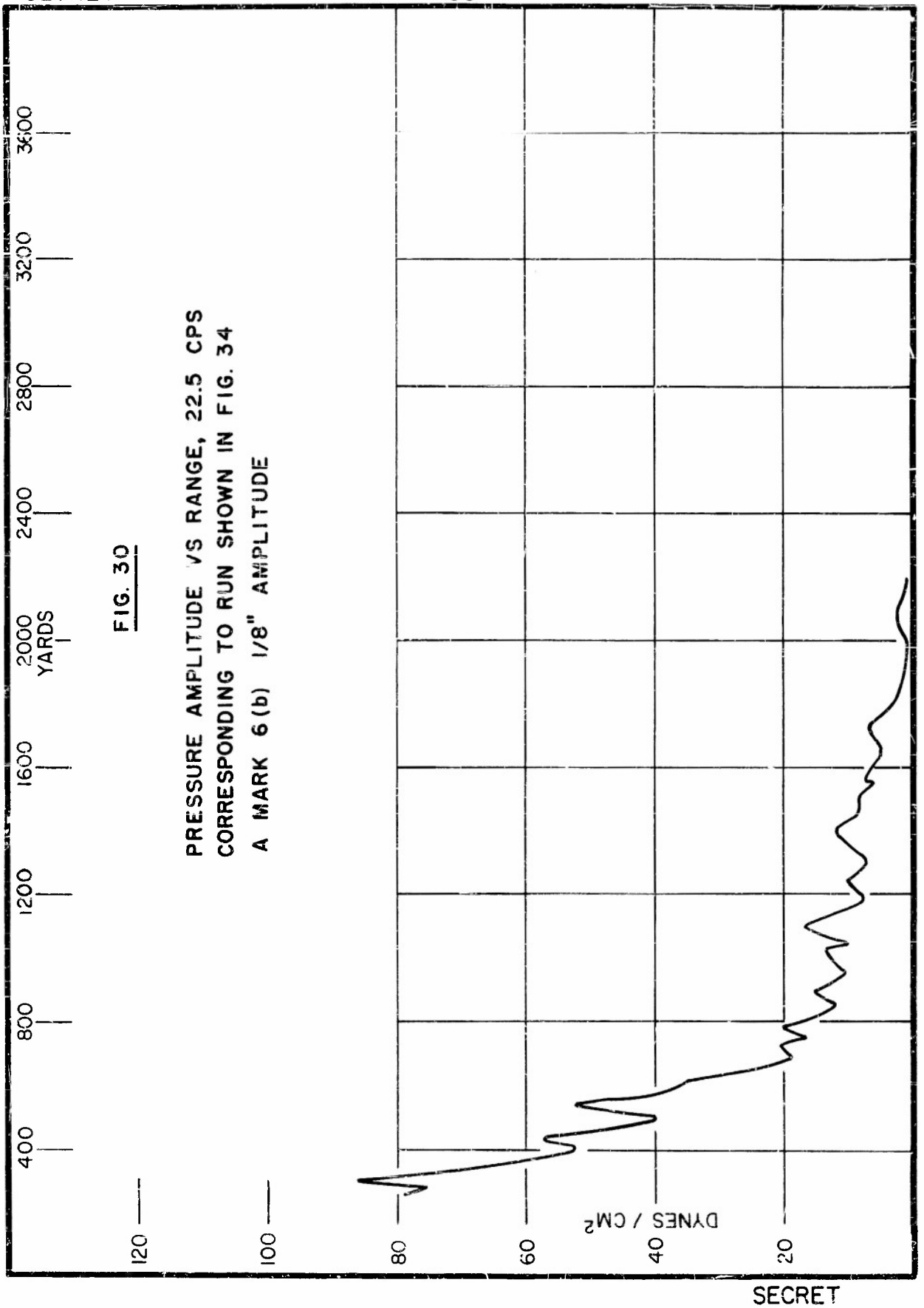


FIG. 30

PRESSURE AMPLITUDE VS RANGE, 22.5 CPS
CORRESPONDING TO RUN SHOWN IN FIG. 34
A MARK 6 (b) 1/8" AMPLITUDE

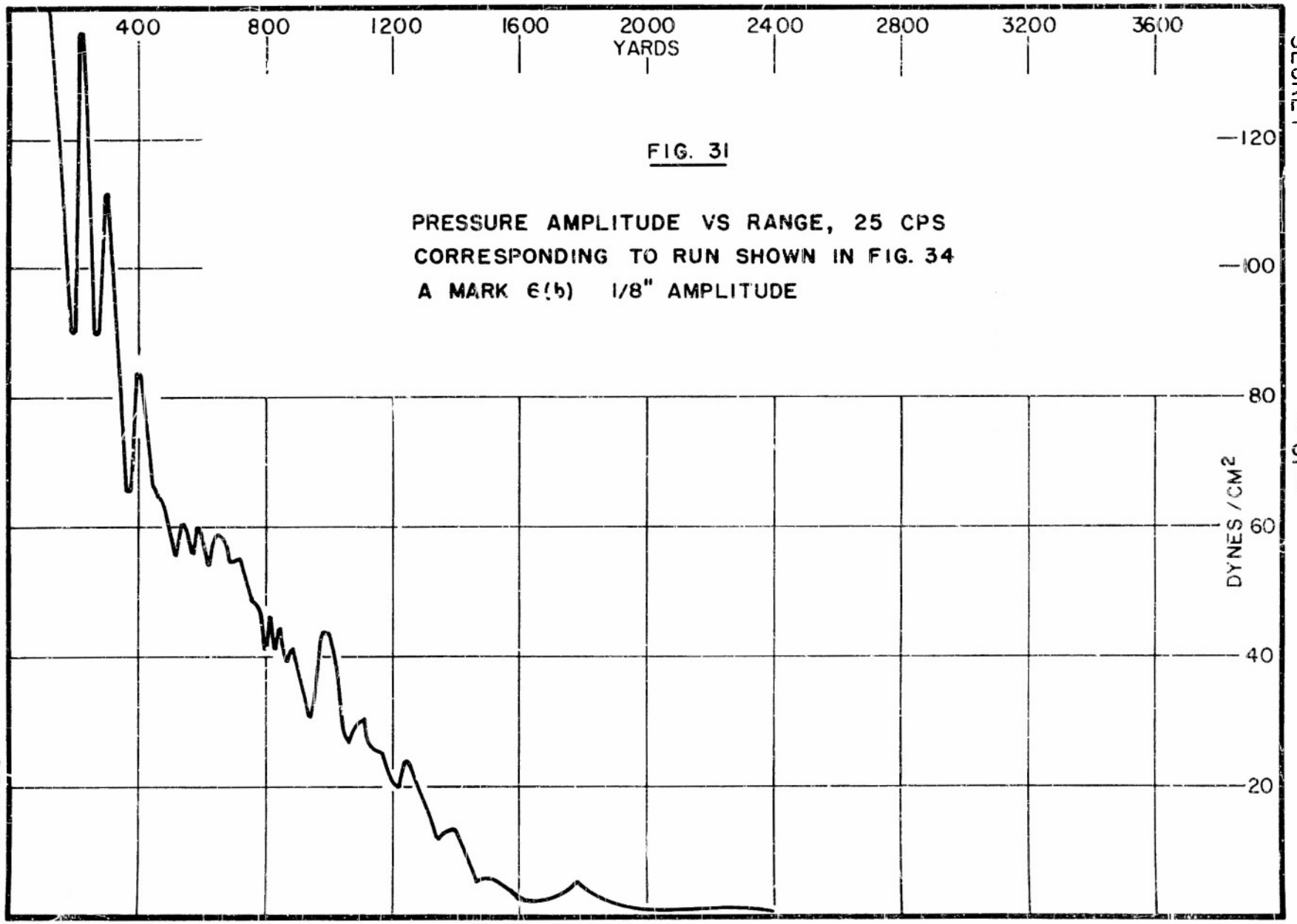


FIG. 31

PRESSURE AMPLITUDE VS RANGE, 25 CPS
CORRESPONDING TO RUN SHOWN IN FIG. 34
A MARK 6(b) 1/8" AMPLITUDE

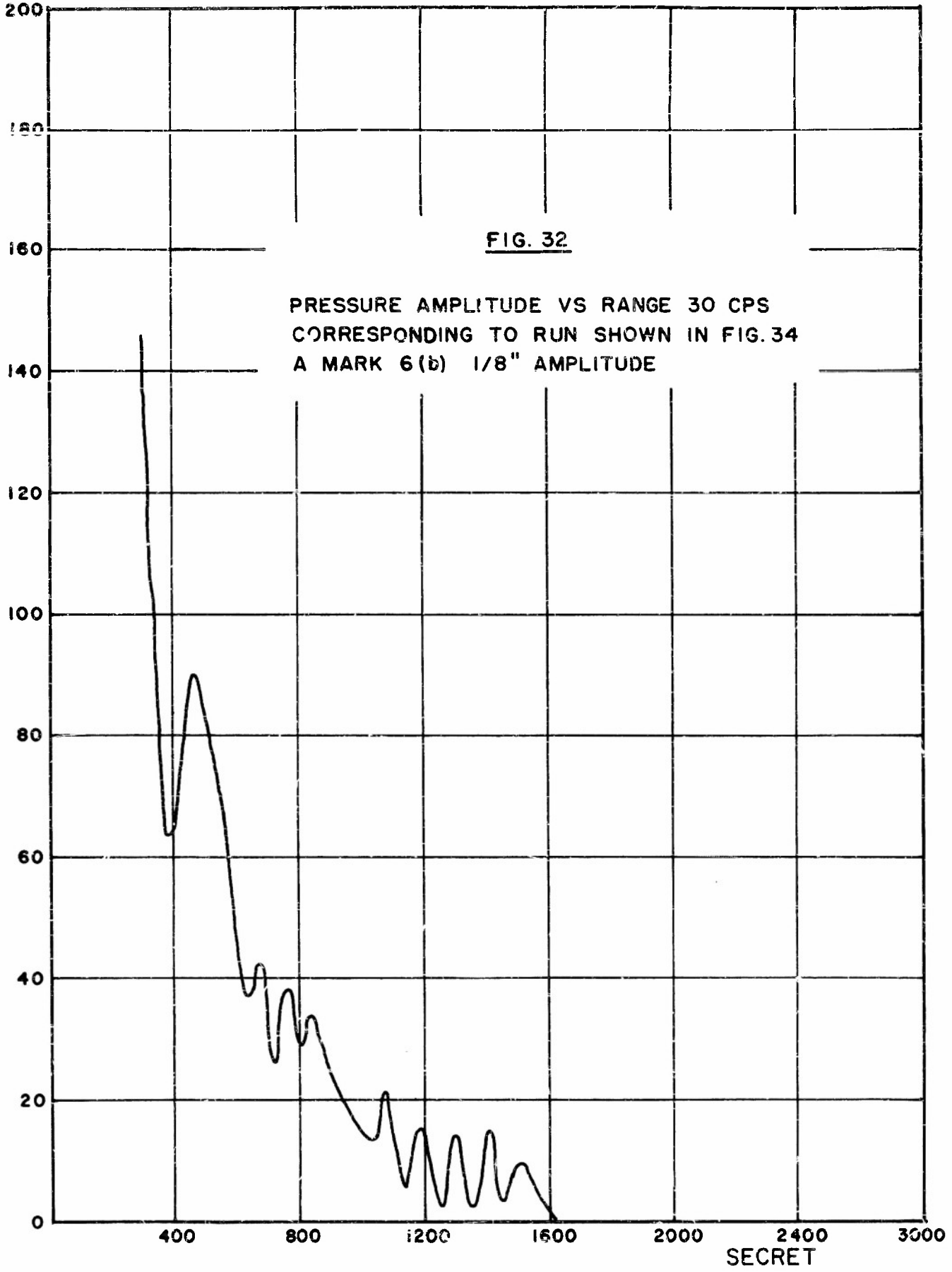


FIG. 32

PRESSURE AMPLITUDE VS RANGE 30 CPS
CORRESPONDING TO RUN SHOWN IN FIG. 34
A MARK 6(b) 1/8" AMPLITUDE

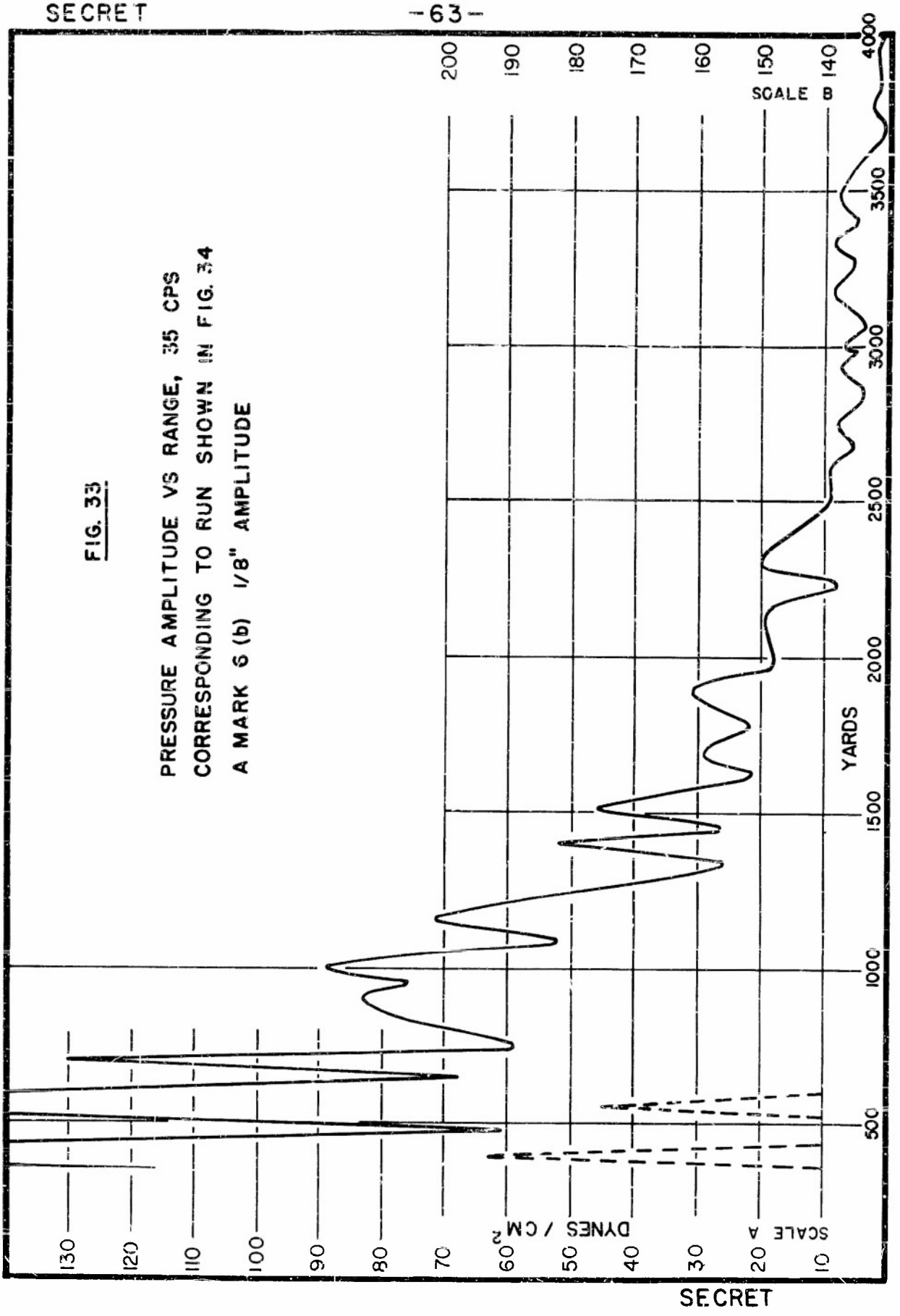


FIG. 33

PRESSURE AMPLITUDE VS RANGE, 35 CPS
CORRESPONDING TO RUN SHOWN IN FIG. 34
A MARK 6 (b) 1/8" AMPLITUDE

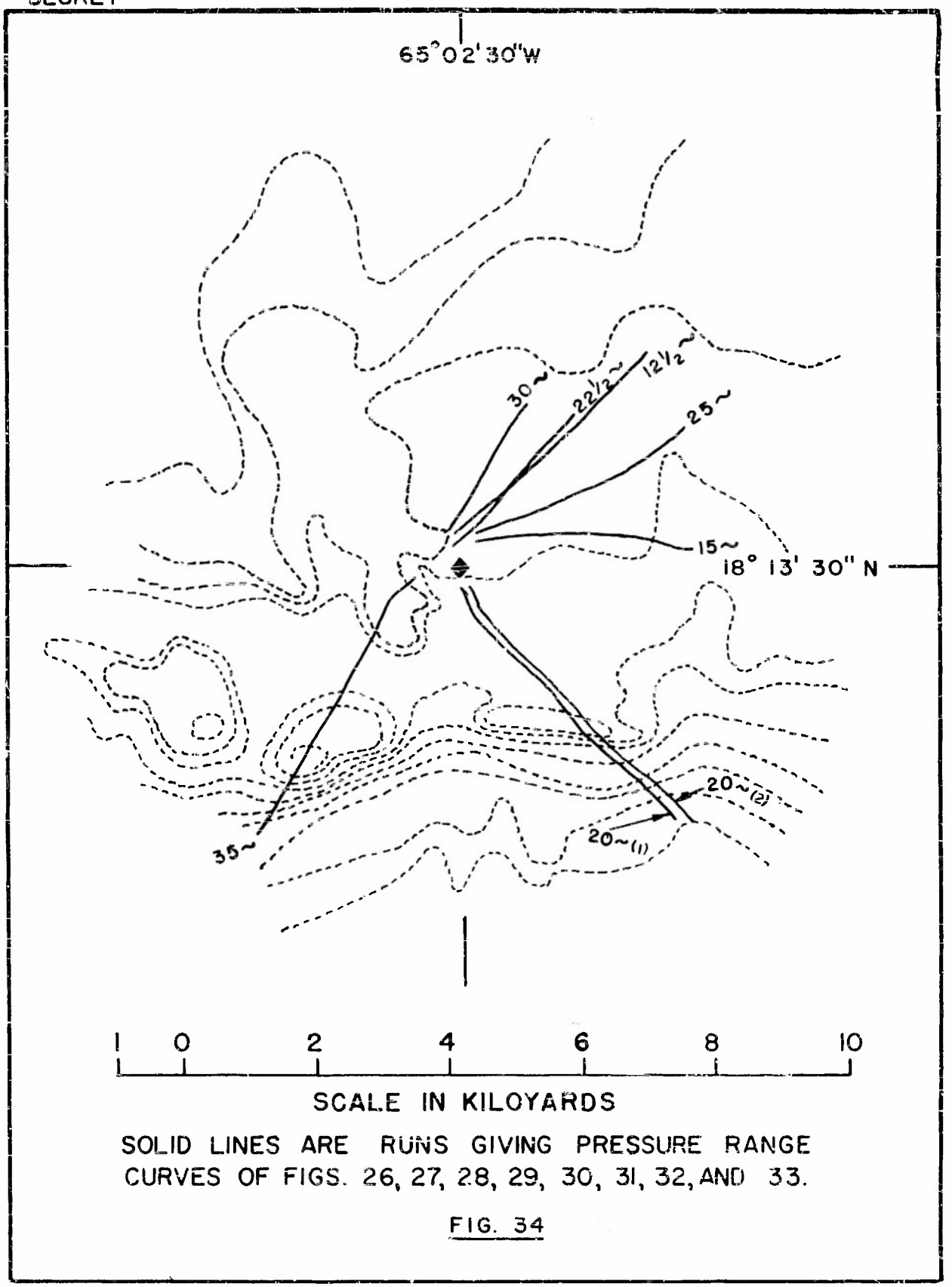


SOLID LINES ARE RUNS GIVING PRESSURE RANGE CURVES OF FIGS. 26, 27, 28, 29, 30, 31, 32, AND 33.

FIG. 34

FIG. 35

PRESSURE LEVEL VS RANGE FOR RUNS INDICATED WITH SOLID LINES IN NE QUADRANT OF FIG. 22

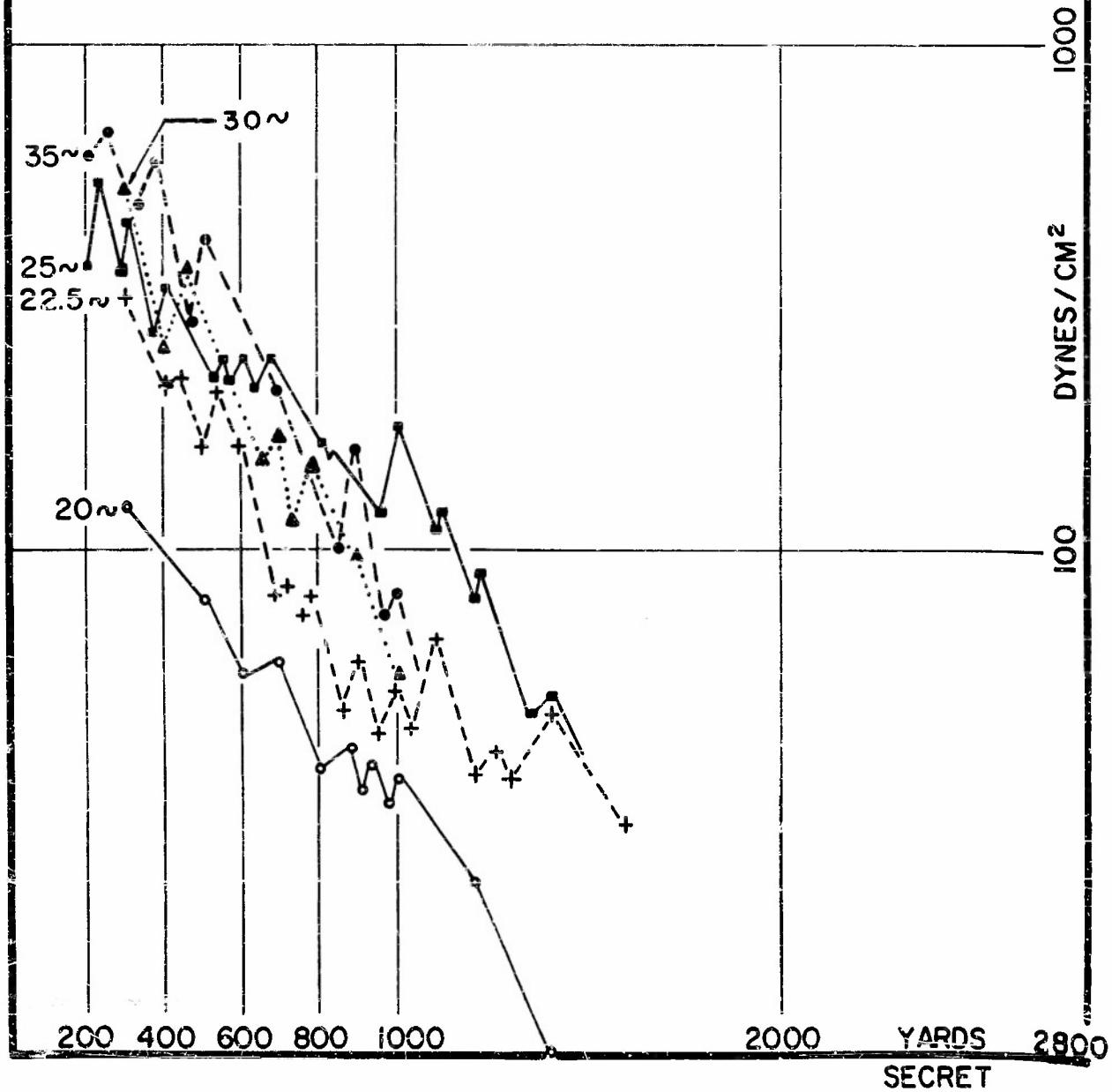

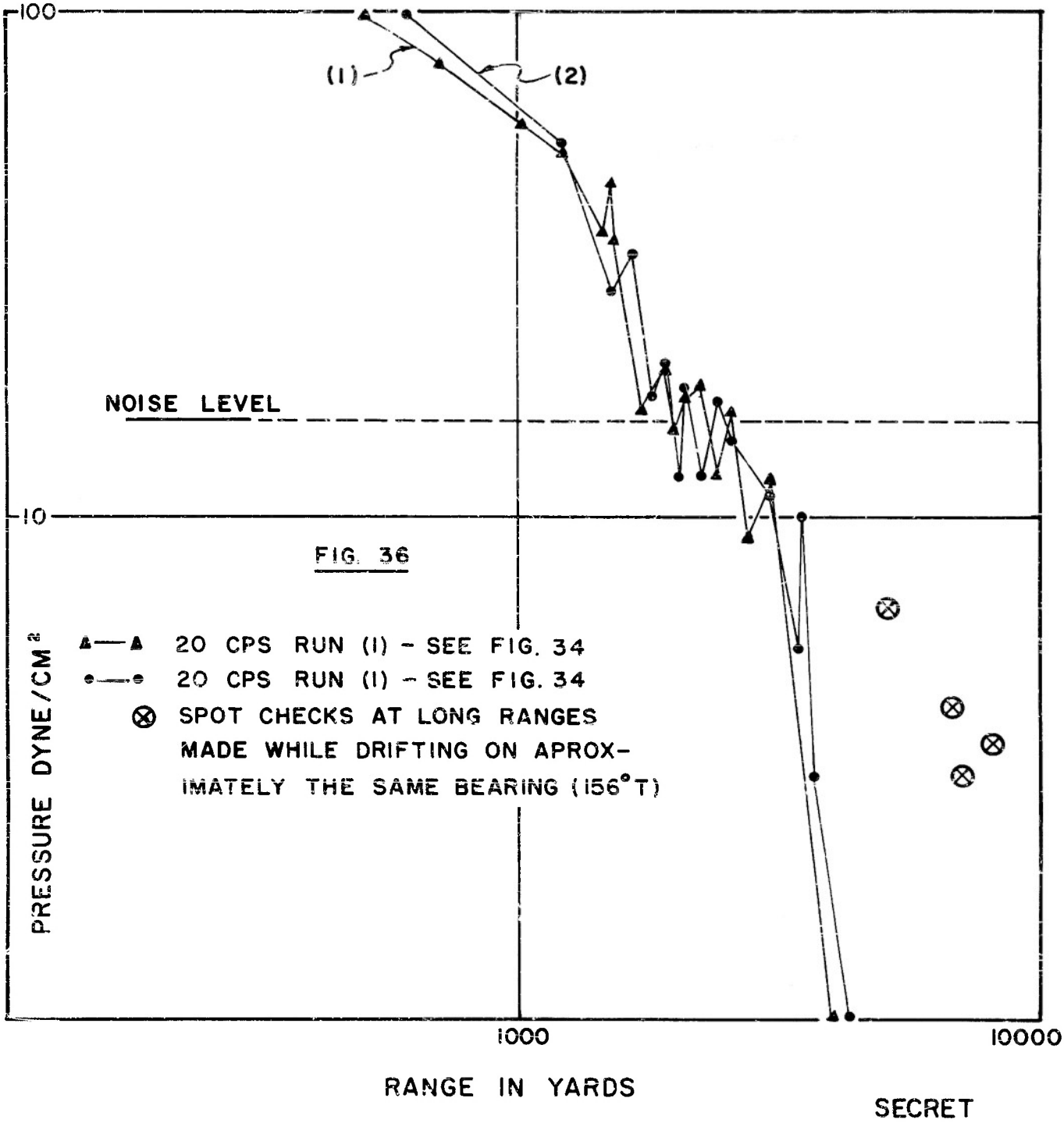
100
10
(1)
(2)
NOISE LEVEL
PRESSURE DYNE/CM²
▲—▲ 20 CPS RUN (1) - SEE FIG. 34
●—● 20 CPS RUN (1) - SEE FIG. 34
⊗ SPOT CHECKS AT LONG RANGES MADE WHILE DRIFTING ON APROX-IMATELY THE SAME BEARING (156°T)
1000
10000
RANGE IN YARDS

FIG. 36

# DISTRIBUTION LIST

## PROJECT MICHAEL TECHNICAL REPORTS

| | COPY NO. |
|---|---|
| Director<br>Naval Research Laboratory (2021)<br>Washington 20, D. C. | 001 |
| Director<br>Naval Research Laboratory<br>Code 1109<br>Washington 20, D. C. | 002 |
| Committee on Undersea Warfare<br>National Research Council<br><br>Via: Contract Administrator<br>Southeast Area<br>Office of Naval Research<br>c/o George Washington University<br>2110 G Street N.W.<br>Washington, D. C. | 003 |
| Commanding Officer and Director<br>U.S. Navy Electronics Laboratory<br>San Diego 52, California | 004 |
| Marine Physical Laboratory<br><br>Via: U.S. Navy Electronics Laboratory<br>Code 1200<br>San Diego, California | 005 |
| Commanding Officer & Director<br>U.S. Navy Underwater Sound Laboratory<br>Fort Trumbull<br>New London, Connecticut | 006 |
| Director<br>U.S. Navy Underwater Sound Reference Laboratory<br>P.O. Box 3629<br>Orlando, Florida | 007 |

## DISTRIBUTION LIST

## PROJECT MICHAEL TECHNICAL REPORTS

| | COPY NO. |
|---|---|
| Commander<br>U. S. Naval Ordnance Laboratory<br>White Oak<br>Silver Spring 19, Maryland | 008 |
| Commander<br>U. S. Naval Air Development Center<br>Johnsville, Pennsylvania | 009 |
| Chief of Naval Operations (Op-316)<br>Navy Department<br>Washington 25, D. C. | 010<br>011 |
| Chief of Naval Operations (Op-31)<br>Navy Department<br>Washington 25, D. C. | 012 |
| Commander, Submarine Force<br>U.S. Atlantic Fleet<br>U.S. Naval Submarine Base<br>Box 27<br>New London, Connecticut | 013 |
| Commander, Submarine Force<br>U.S. Pacific Fleet<br>Fleet Post Office<br>San Francisco, California | 014 |
| Commanding Officer & Director<br>David Taylor Model Basin<br>Washington 7, D. C.<br>Att: Mr. Lasky | 015 |
| Commanding General<br>Headquarters, Air Force<br>Washington 25, D. C. | 016 |

## DISTRIBUTION LIST

## PROJECT MICHAEL TECHNICAL REPORTS

| | COPY NO. |
|---|---|
| Commanding Officer<br>Signal Corps Engineering Laboratory<br>Squier Signal Laboratory<br>Fort Monmouth, New Jersey | 017 |
| Commander<br>U.S. Naval Ordnance Test Station<br>Pasadena Annex<br>3202 E. Foothill Boulevard<br>Pasadena 8, California | 018 |
| Chief, Bureau of Ships (Code 845)<br>Navy Department<br>Washington 25, D. C. | 019 |
| Chief, Bureau of Ships (Code 520)<br>Navy Department<br>Washington 25, D. C. | 020 |
| Chief, Bureau of Ships (Code 371)<br>Navy Department<br>Washington 25, D. C. | 021 |
| Chief, Bureau of Ships (Code 849)<br>Navy Department<br>Washington 25, D. C. | 022 |
| Chief, Bureau of Ships (Code 847)<br>Navy Department<br>Washington 25, D. C. | 023 |
| Chief, Bureau of Aeronautics (EL 46)<br>Navy Department<br>Washington 25, D. C. | 024 |

## DISTRIBUTION LIST

## PROJECT MICHAEL TECHNICAL REPORTS

| | COPY NO. |
|---|---|
| Chief, Bureau of Ordnance<br>Navy Department<br>Washington 25, D. C. | 025 |
| Commander-in-Chief<br>U.S. Atlantic Fleet<br>U.S. Naval Station<br>Norfolk 11, Virginia | 026 |
| Commander, Operational Development Force<br>U.S. Atlantic Fleet<br>U.S. Naval Base<br>Norfolk 11, Virginia | 027 |
| Commander-in-Chief<br>U.S. Pacific Fleet<br>Fleet Post Office<br>San Francisco, California | 028 |
| Commander, Submarine Development Group Two<br>U.S. Naval Submarine Base<br>Box 70<br>New London, Connecticut | 029 |
| Commanding Officer<br>Office of Naval Research Branch Office<br>1030 E. Green Street<br>Pasadena, California | 030 |
| Commanding Officer<br>Office of Naval Research Branch Office<br>1000 Geary Street<br>San Francisco, California | 031 |
| Commanding Officer<br>Office of Naval Research Branch Office<br>86 E. Randolph Street<br>Chicago 1, Illinois | 032 |

## DISTRIBUTION LIST

## PROJECT MICHAEL TECHNICAL REPORTS

| | COPY NO. |
|---|---|
| Mr. R. N. Hamme<br>3039 Randall Laboratory<br>Engineering Research Institute<br>University of Michigan<br>Ann Arbor, Michigan | 033 |
| Dr. J. R. Frederick<br>Engineering Research Institute<br>University of Michigan<br>Ann Arbor, Michigan<br><br>Via: Office of Naval Research Branch office<br>86 E. Randolph Street<br>Chicago 1, Illinois | 034 |
| Commander<br>Surface Antisubmarine Development Detachment<br>U.S. Naval Station<br>Key West, Florida | 035 |
| Officer-in-Charge<br>Office of Naval Research Branch Office<br>Navy #100<br>FPO New York, New York | 036 |
| Commanding Officer<br>Office of Naval Research Branch Office<br>346 Broadway<br>New York 13, New York | 037 |
| Edwards Street Laboratory<br>Yale University<br>Box 1916, Yale Station<br>New Haven, Connecticut<br>Via: ONR, New York | 038 |
| Bell Telephone Laboratories<br>Murray Hill<br>New Jersey<br>Via: ONR, New York | 039 |

# DISTRIBUTION LIST

## PROJECT MICHAEL TECHNICAL REPORTS

| | | COPY NO. |
|---|---|---|
| Bell Telephone Laboratories<br>Whippany<br>New Jersey | Via: ONR, New York | 040 |
| Lamont Geological Observatory<br>Torrey Cliff<br>Palisades, New York | Via: ONR, New York | 041 |
| Commanding Officer<br>Office of Naval Research Branch Office<br>150 Causeway Street<br>Boston, Massachusetts<br>Att: Dr. F. V. Hunt | | 042 |
| Research Analysis Group<br>Brown University<br>Providence, Rhode Island | Via: ONR, Boston | 043 |
| Director<br>Woods Hole Oceanographic Institution<br>Woods Hole, Massachusetts<br>Att: Dr. J. B. Hersey | Via: ONR, Boston | 044 |
| Head, Undersea Warfare Branch<br>Office of Naval Research, Code 466<br>Washington 25, D. C.<br>Att: LCDR W. W. Upshaw, USN | | 045 through 058 |